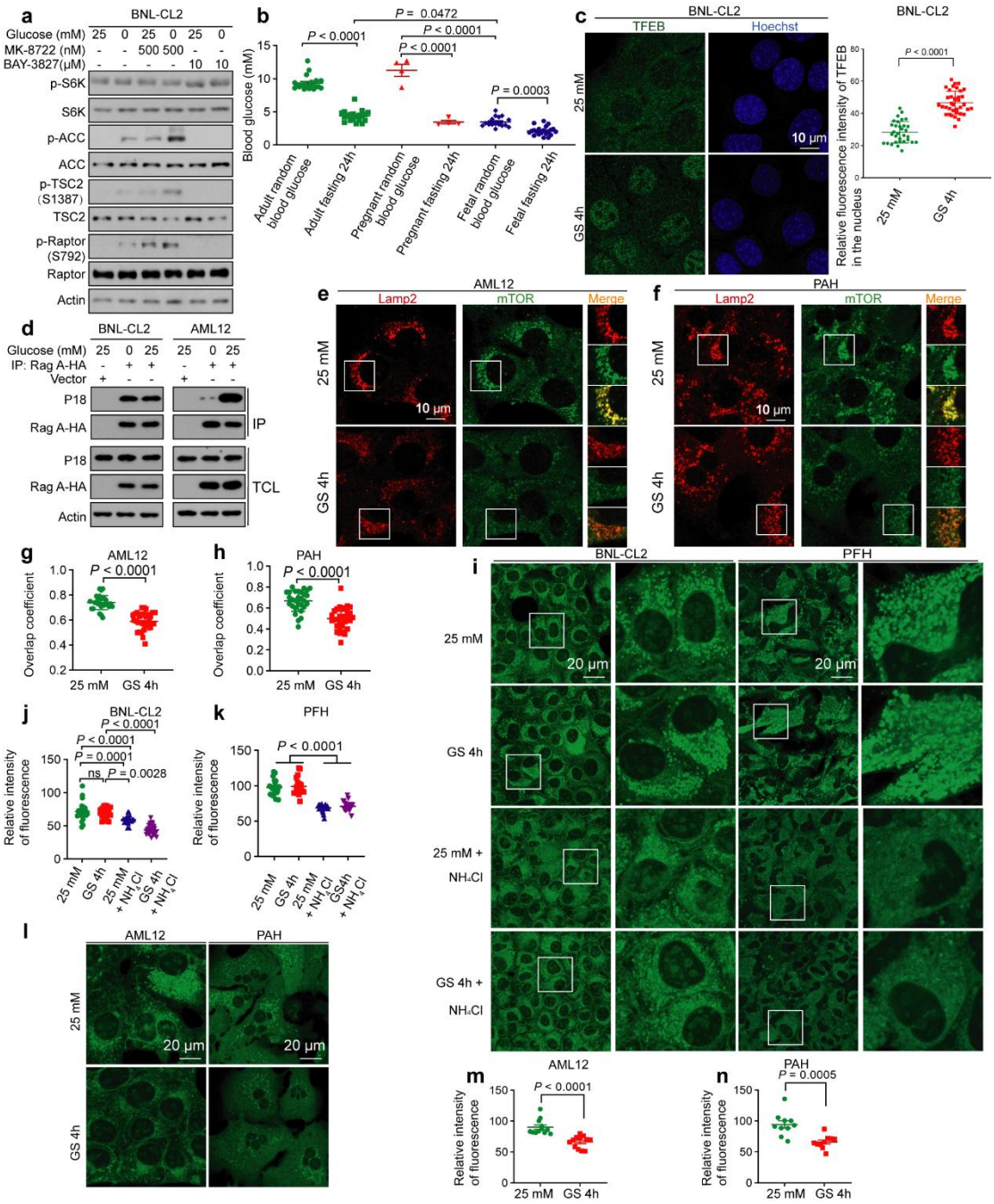

Fig. S1. mTORC1 remains active in fetal hepatocytes in low glucose, but not in adult hepatocytes, related to Fig. 1 and Fig. 2.

a mTORC1 remains active when treated with AMPK activator MK-8722 or inhibitor BAY-3827 in BNL-CL2, followed by determining p-S6K levels by immunoblotting. **b** Fasted pregnant mice (fetuses of E18.5d) and 8-week female adult mice showed a

significant decrease of plasma glucose after 24 h fasting (from 9.3 to 4.4 mM in the adults, from 11.3 to 3.5 mM in the pregnant mice, and from 3.5 to 2.1 mM in the fetus). Blood samples were collected from adult mice (8-week-old; adult blood glucose), pregnant mice (E18.5d; pregnant blood glucose), or embryos (E18.5d; fetal blood glucose), after being fasted for 0 h or 24 h. Blood glucose levels were detected by a portable human glucometer (Accu-Chek; Roche). Data are presented as mean ± SEM, n = 20 for each adult group of **b**, n = 4 for each pregnant group of **b**, n = 16 for fetal random blood glucose group of **b**, n = 21 for fetal fasting 24 h group of **b,** with P values calculated using two-way ANOVA, followed by Tukey. **c** The TFEB is translocated into nucleus after starvation for 4 h detected by immunofluorescence and the relative fluorescence intensity were shown (presented as mean ± SEM, 25 mM n = 32, 0 mM n = 37, with P values calculated using unpaired two-tailed Student's t-test). **d** mTORC1 remains associated with RAG in BNL-CL2 in low glucose. See also AML12 cells, as a control, in which mTORC1 is not associated with RAG. **e**–**h** mTORC1 dissociates from the lysosomes in low glucose conditions in adult hepatocytes. The AML12 adult hepatocyte cell line (**e**, **g**) and primary adult hepatocytes (**f**, **h**) were glucose-starved for 4 h. Endogenous mTOR (labelled in green with rabbit anti-mTOR antibody, CST 2983T) and the lysosome marker LAMP2 (labelled in red with rat anti-LAMP2 antibody, Abcam AB13524) were then stained. Representative images are shown in **e** and **f**, and the Pearson's overlap coefficients in **g** and **h** (presented as mean ± SEM, 25 mM n = 28, 0 mM n = 33 of **g** or 25 mM n = 29, 0 mM n = 30 of **h**, with P values calculated using unpaired two-tailed Student's t-test). **i**–**n** Glucose starvation does not affect the

lysosomal acidity in fetal hepatocytes. The BNL-CL2 (left panel of **i**, and **j**), primary fetal hepatocytes (right panel of **i**, and **k**), AML12 (left panel of **l**, and **m**), and primary adult hepatocytes (right panel of **l**, and **n**) were either glucose-starved for 4 h or treated with 25 mM NH_4Cl, the lysosome inhibitor, as a control for 2 h. In contrast, low glucose effectively inhibited v-ATPase in adult hepatocytes. The cells were incubated with 1 μM Lysosensor^{TM} Green DND-189 (Thermo L7535) for 30 min to detect the PH of lysosomes. Representative images are shown in **i** and **l**, and the Mander's overlap coefficients in **j**, **k**, and **m**, **n** (presented as mean ± SEM, $n = 25$ for 25 mM group of **j**, $n = 22$ for 0 mM group of **j**, $n = 21$ for 25 mM + NH_4Cl group of **j**, $n = 24$ for 0 mM + NH_4Cl group of **j**; $n = 19$ for each group of **k**, with P values calculated using two-way ANOVA, followed by Tukey. $n = 12$ for each group of **m**, $n = 10$ for each group of **n**, with P values calculated using unpaired two-tailed Mann-Whitney test (**m**), or unpaired two-tailed Student's t-test (**n**)). The original western blots with protein ladder are shown in Supplementary Data S1. ns, not significant ($P > 0.05$).

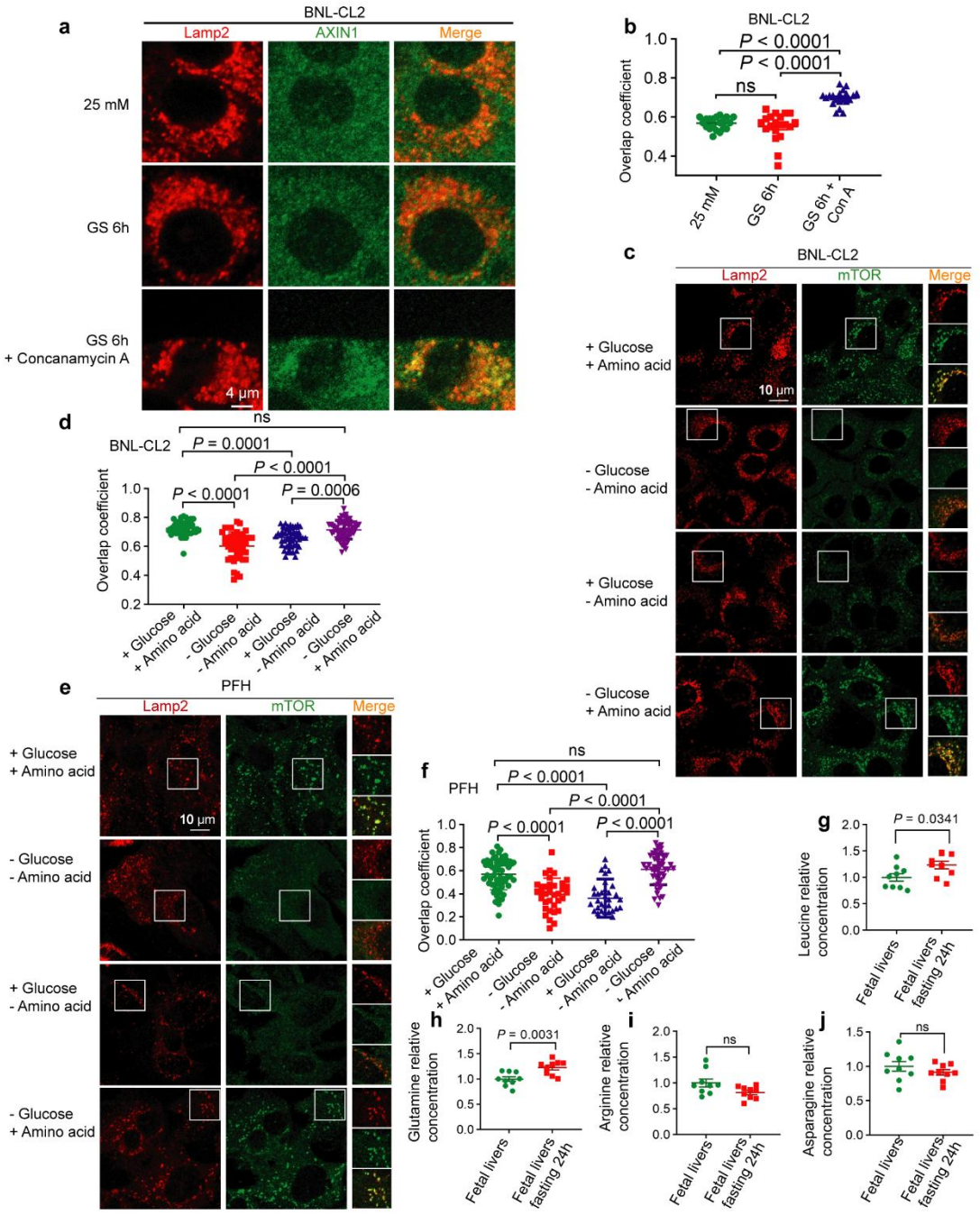

Fig. S2. Constitutively active v-ATPase-Ragulator-RAG axis maintains mTORC1 activity in fetal hepatocytes in low glucose, related to Fig. 2.

a, **b** Forced inhibition of v-ATPase in fetal hepatocytes by concanamycin A (conA) effectively triggers the lysosomal translocation of AXIN. BNL-CL2 were either

glucose-starved or treated with 1μM Concanamycin A, the v-ATPase inhibitor, as a control for 6 h. Endogenous AXIN1 (labeled in green with goat anti-AXIN1 antibody, Santa Cruz Biotechnology SC-8567) and the lysosome marker LAMP2 (labeled in red with rat anti-LAMP2 antibody, Abcam AB13524) were then stained. Representative images are shown in **a**, and the Mander's overlap coefficients in **b** (presented as mean ± SEM, n = 20 for each group, with P values calculated using two-way ANOVA, followed by Tukey). **c**–**f** mTORC1 dissociates from the lysosomes in amino acid deficiency conditions in fetal hepatocytes. The BNL-CL2 (**c**, **d**) and primary fetal hepatocytes (**e**, **f**) were either glucose-starved or amino acid-starved for 2 h. Endogenous mTOR (labeled in green with rabbit anti-mTOR antibody, CST 2983T) and the lysosome marker LAMP2 (labeled in red with rat anti-LAMP2 antibody, Abcam AB13524) were then stained. Representative images are shown in **c** and **e**, and the Pearson's overlap coefficients are shown in D and F (presented as mean ± SEM, n = 41 for + Glucose + Amino acid group of **d**, n = 41 for - Glucose - Amino acid group of **d**, n = 51 for + Glucose - Amino acid group of *d*, n = 56 for - Glucose + Amino acid group of **d**; n = 58 for + Glucose + Amino acid group of **f**; n = 35 for - Glucose - Amino acid group of **f**; n = 33 for + Glucose - Amino acid group of **f**; n = 48 for - Glucose + Amino acid group of **f**, with P values calculated using two-way ANOVA, followed by Tukey). **g**–**j** Maternal fasting does not decrease the levels of amino acids, such as leucine, glutamine, arginine, and asparagine, all of which can regulate mTORC1 activity, in the fetal liver. Liver tissues were collected from E18.5d fetal mice after the pregnant females were fasted for 0 h or 24 h, followed by determination of amino acid levels

through HPLC-MS analysis. Fasting did not decrease the relative concentration of leucine (**g**), glutamine (**h**), arginine (**i**), and asparagine (**j**) in fetal liver tissues between the fasting and control groups (presented as mean ± SEM, $n = 9$ for each group of **g**–**j**, with P values calculated using unpaired two-tailed Student's t-test). ns, not significant ($P > 0.05$).

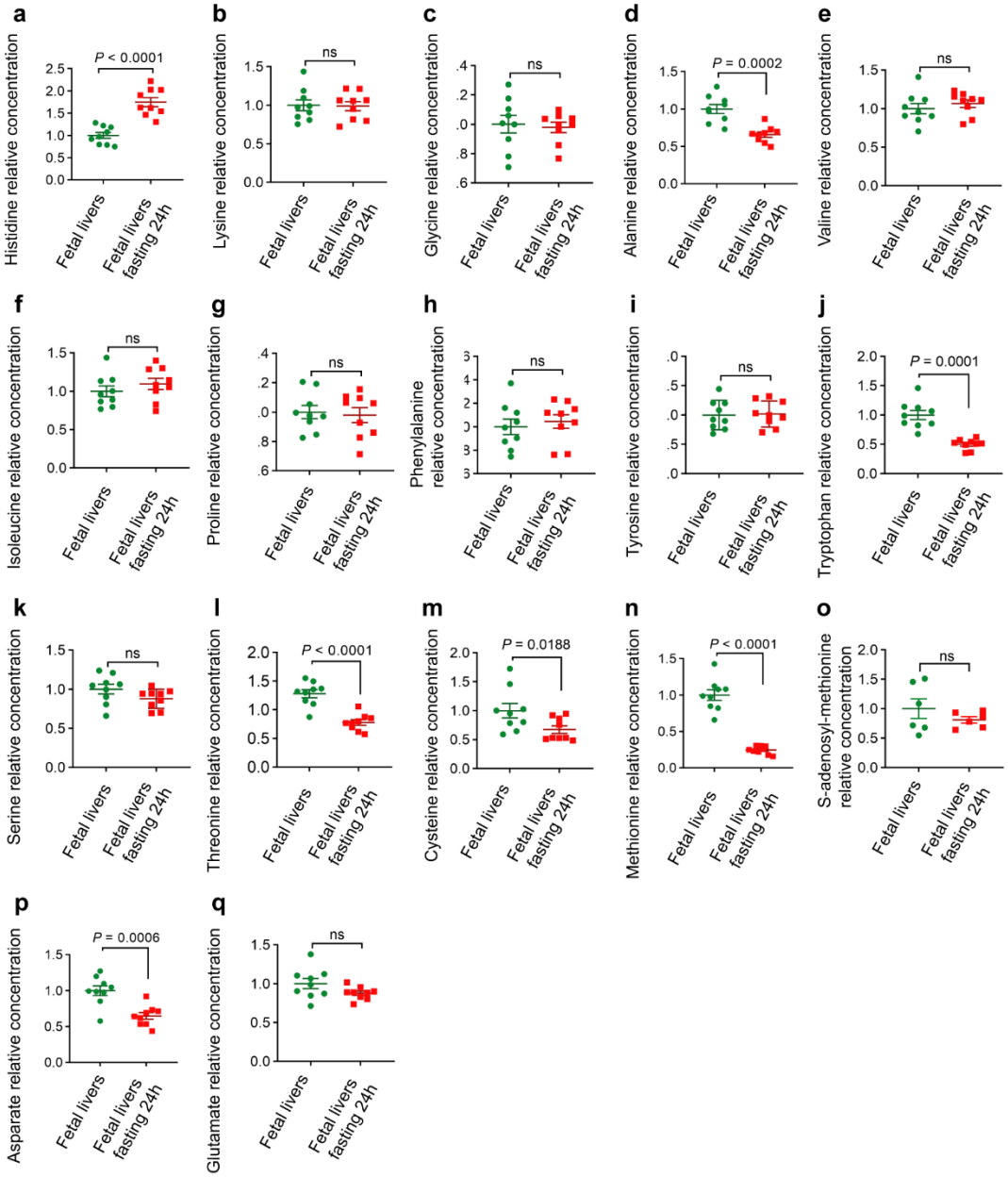

75

76 **Fig. S3. The overall levels of most amino acids in the liver of E18.5 d fetal mice do**

77 **not significantly change after the pregnant females being fasted, related to Fig. 2.**

78 **a–q** Liver tissues were collected from E18.5d fetal mice after the pregnant females were

79 fasted for 0 h or 24 h, followed by the detection of the relative concentration of histidine

80 (**a**), lysine (**b**), glycine (**c**), alanine (**d**), valine (**e**), isoleucine (**f**), proline (**g**),

81 phenylalanine (**h**), tyrosine (**i**), tryptophan (**j**), serine (**k**), threonine (**l**), cystine (**m**),

methionine (**n**), s-adenosyl-methionine (**o**), asparate (**p**), glutamate (**q**) in fetal liver tissues between the fasting and control groups using HPLC-MS (presented as mean ± SEM, $n = 9$ for each group of **a**–**n**, **p**, **q**, except $n = 6$ for each group of **o**, with P values calculated using unpaired two-tailed Student's t-test (**a-i**, **k-l**, **p**), or unpaired t test with Welch's correction (**j**, **n**, **o**, **q**), or unpaired two-tailed Mann-Whitney test (**m**)). ns, not significant ($P > 0.05$).

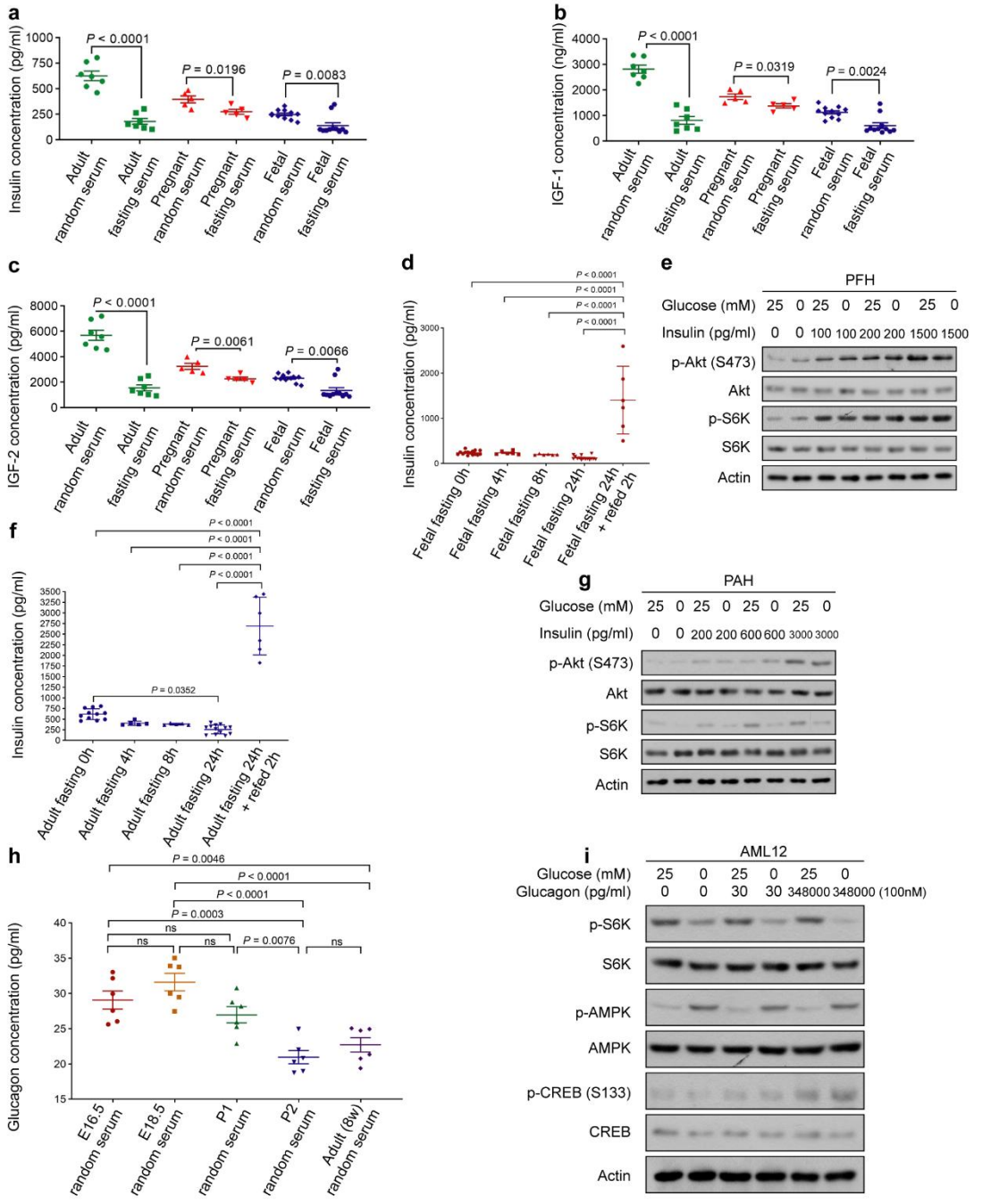

Fig. S4. Effects of physiological concentrations of insulin and glucagon on Akt and mTORC1, related to Fig. 2 and Fig. 3.

a–**g** Maternal fasting does not inhibit AKT signaling in fetal livers. Adult mice or pregnant mice were fasted for 24 h and the insulin (**a**), IGF-1 (**b**), and IGF-2 (**c**)

concentrations in the serum of the fetuses were checked by ELISA. Fetal mice (E18.5d) insulin (**d**) and the p-AKT levels in primary fetal hepatocytes (**e**) were also detected in a series of fasted time (0, 4, 8 and 24 h) and refed group (fasted for 24 h followed refed 2 h was defined as refed group). Data in **a**–**d** are shown as mean ± SEM; n = 7 (adult mice of **a**–**c**), 5 (pregnant mice of **a**–**c**), or 11 (fetal mice of **a**–**c**) mice for each condition, with P values calculated using unpaired two-tailed Student's t-test (**a**–**c**), except for fetal mice (**a**–**c**) where unpaired two-tailed Mann-Whitney test is used. For **d**, fetal mice fasting 0 h and 24 h: n = 15; other fetal mice groups with different fasting time: n =6 , with P values calculated using two-way ANOVA, followed by Tukey. For **f**, adult fasting 0 h: n = 11; adult fasting 4 h and 8 h: n = 5: adult fasting 24 h: n = 13, adult refed: n = 6, with P values calculated using two-way ANOVA, followed by Tukey. **h** The glucagon concentration was detected at various developmental stages by ELISA. Data are shown as mean ± SEM; n = 6 in each group, with P values calculated by one-way ANOVA, followed by Tukey. **i** Adding physiological concentration of glucagon (30 pg/mL) and ultra-high glucagon (100 nM) to AML12, and giving corresponding glucose starvation treatment for 4 h, mTORC1 of AML12 still showed sensitivity to low glucose. The original western blots with protein ladder are shown in Supplementary Data S1. ns, not significant ($P > 0.05$).

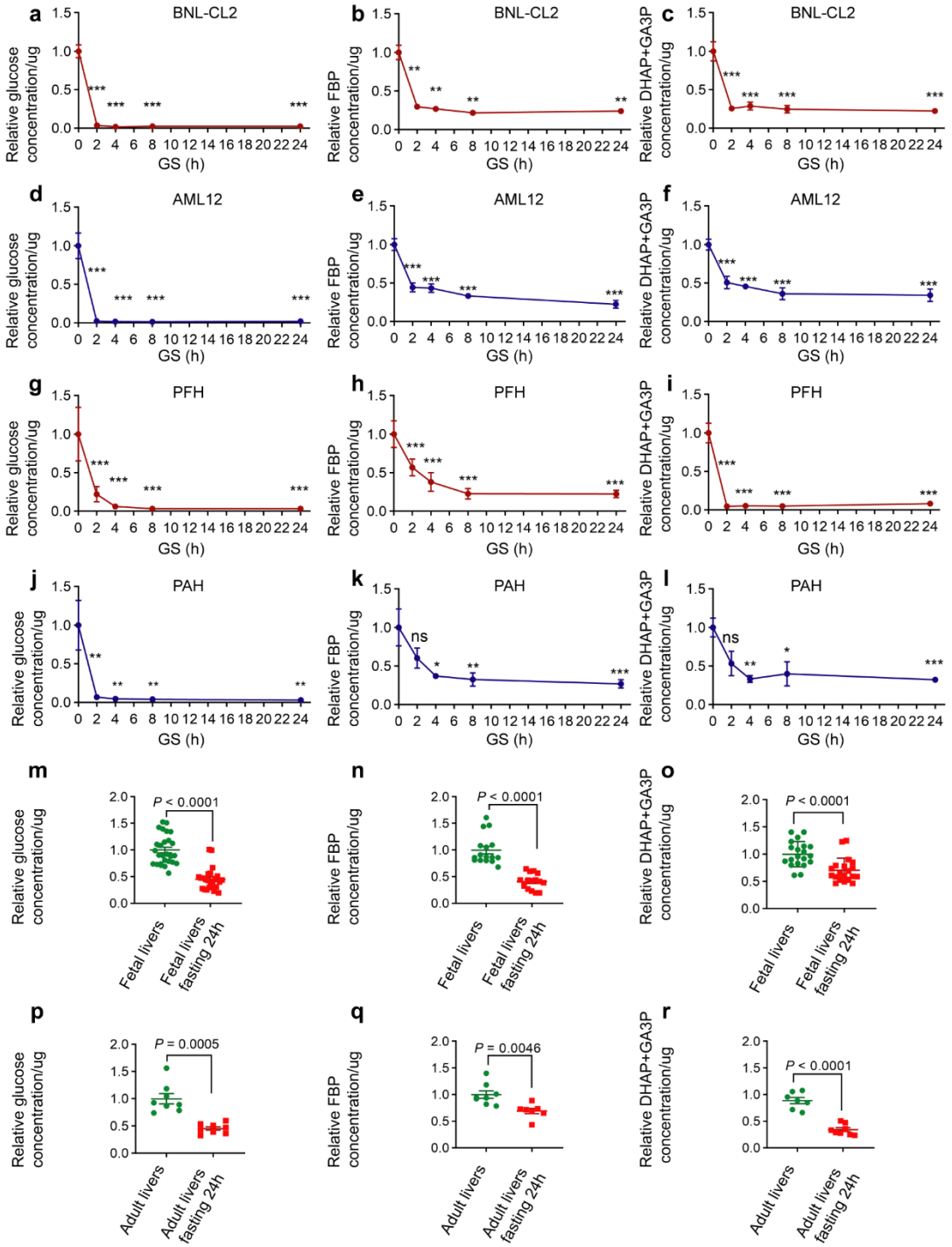

111

112 **Fig. S5. FBP and DHAP decrease in the fetal liver and adult livers in low glucose,**

113 **related to Fig. 3.**

114 **a**–**l** Levels of FBP and DHAP are decreased in both fetal hepatocytes and adult

115 hepatocytes in low glucose. BNL-CL2 (a–c), AML12 (d–f), PFH (g–i), and PAH (j–l)

were glucose-starved for 0 hour, 2 h, 4 h, 8 h, or 24 h, followed by determination of FBP and DHAP by HPLC-MS. Data are presented as mean ± SEM, n = 5 for each condition of **a**–**f**, n = 4 for each condition of **g**–**i**, n = 6 for each condition of **j**–**l**, except n = 3 for PFH 0 hour group of **g**–**i**. P values were calculated using one-way ANOVA, followed by Dunnett's T3 multiple comparisons test (**a**–**d**, **j**), or followed by Dunnett's multiple comparisons test (**e**–**i**); or using Kruskal-Wallis test, followed by Dunn's multiple comparisons test (**k**, **l**). * P <0.05, ** P <0.01, *** P <0.001, all compared with 0 hour group. **m**–**r** Levels of FBP and DHAP are decreased in the liver tissues of fetal mice after maternal fasting (**m**–**o**), or in adult mouse livers (**p**–**r**). Liver tissues were collected from pregnant mice embryos (E18.5 d; fetal liver tissue) or adult mice (8-week-old; adult liver tissue), after being fasted for 0 h or 24 h. FBP and DHAP were determined by HPLC-MS in liver tissue. Data are presented as mean ± SEM. n = 27 for fetal livers group of **m**, n = 24 for fetal livers fasting 24 h group of **m**; n = 16 for each group of **n**, n = 20 for each group of **o**, n = 8 for each group of **p**; n = 8 for adult livers group of **q**, n = 7 for adult livers fasting 24 h group of **q**; n = 7 for adult livers group of **r**, n = 8 for adult livers fasting 24 h group of **r**; with P values calculated using unpaired two-tailed Student's t-test (**q**, **r**), or unpaired t test with Welch's correction (**p**), or unpaired two-tailed Mann-Whitney test (**m**–**o**). ns, not significant (P > 0.05).

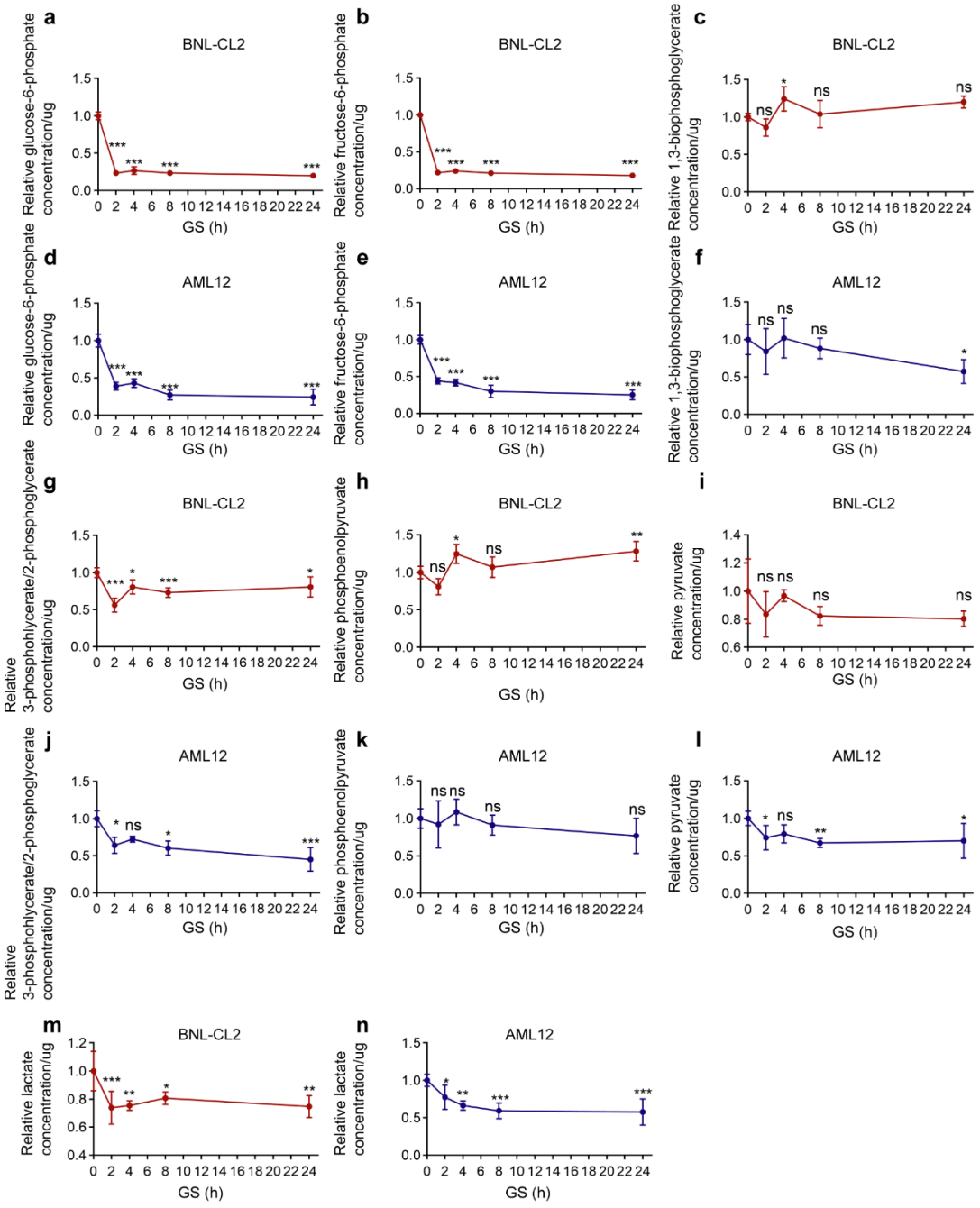

135

136 **Fig. S6. Changes of glycolytic intermediates, other than FBP and DHAP, in hepatic**

137 **cell lines after glucose starvation, related to Fig. 3.**

138 **a**–**n** The changes of glycolytic intermediates, other than FBP and DHAP, in BNL-CL2

139 and AML12 cells after glucose starvation are shown. BNL-CL2 (**a**–**c**, **g**–**i**, **m**) and

140 AML12 (**d**–**f**, **j**–**l**, **n**) cells were glucose-starved for 0 h, 2 h, 4 h, 8 h, or 24 h. HPLC

was used to determine glycolytic intermediates in these cells. Data are presented as mean ± SEM, $n = 5$ for each condition of **a**–**n**. *P* values were calculated using one-way ANOVA, followed by Dunnett's T3 multiple comparisons test (**a**, **i**), or followed by Dunnett's multiple comparisons test (**b**–**h**, **l**–**n**); or using Kruskal-Wallis test, followed by Dunn's multiple comparisons test (**j**, **k**). **P* <0.05; ***P* <0.01; ****P* <0.001; all compared with 0 h group. ns, not significant (*P* > 0.05)

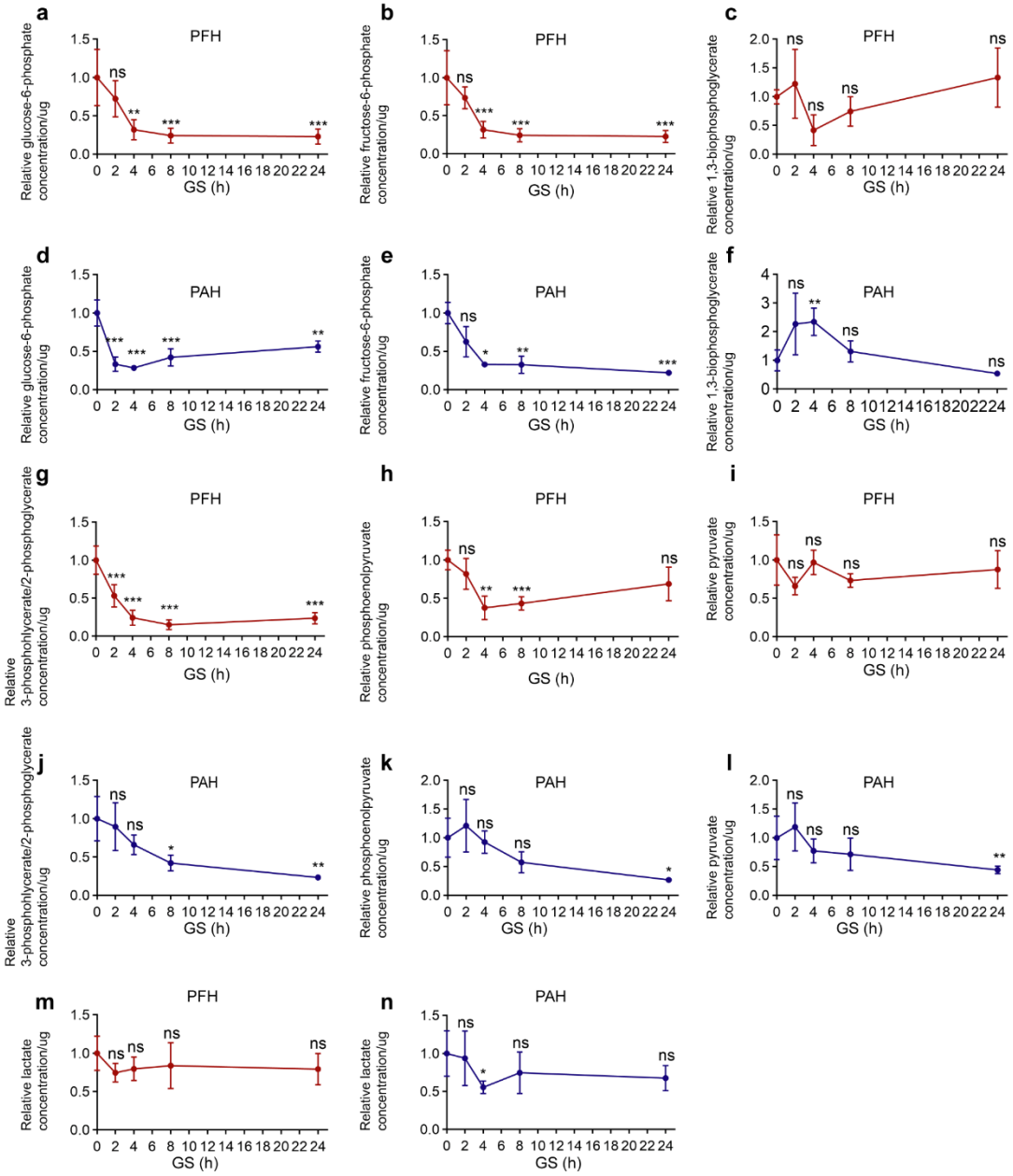

147

148 **Fig. S7. Changes of glycolytic intermediates, other than FBP and DHAP, in**

149 **primary hepatocytes after glucose starvation, related to Fig. 3.**

150 **a**–**n** The changes of glycolytic intermediates, other than FBP and DHAP, in PFH and

151 PAH cells after glucose starvation are shown. PFH (**a**–**c**, **g**–**i**, **m**) and PAH (**d**–**f**, **j**–**l**, **n**)

152 cells were glucose-starved for 0 h, 2 h, 4 h, 8 h, or 24 h. HPLC was used to determine

153 glycolytic intermediates in these cells. Data are presented as mean ± SEM, n = 4 for

each condition of **a**–**c**, **g**–**i**, **m**, $n = 6$ for each condition of **d**–**f**, **j**–**l**, **n**, except $n = 3$ for PFH 0 h group of **a**–**c**, **g**–**i**, **m**. *P* values were calculated using one-way ANOVA, followed by Dunnett's T3 multiple comparisons test (**d**, **f**, **j**, **k**), or followed by Dunnett's multiple comparisons test (**a**, **b**, **g-i**, **n**); or using Kruskal-Wallis test, followed by Dunn's multiple comparisons test (**c**, **e**, **l**, **m**). **P* <0.05; ***P* <0.01; ****P* <0.001; all compared with 0 h group. ns, not significant (*P* > 0.05).

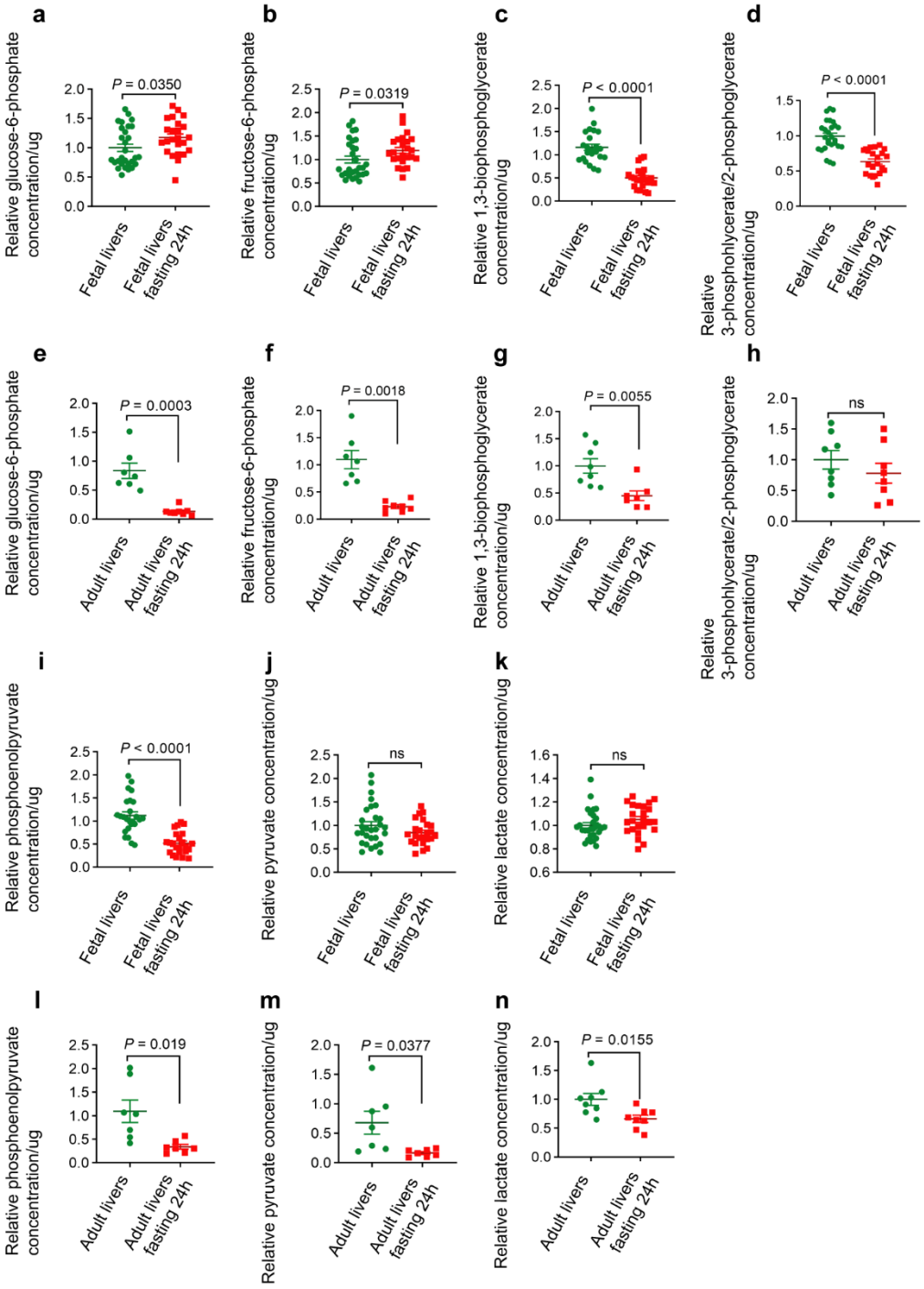

160

161 **Fig. S8. Changes of glycolytic metabolites, other than FBP and DHAP, in the livers**

162 **of E18.5 d fetal mice after the pregnant females being fasted, related to Fig. 3.**

163 **a**–**n** Liver tissues collected from pregnant mouse embryos (E18.5d; fetal liver tissue)

164 or adult mice (8-week-old; adult liver tissue) after fasting for 0 h or 24 h were subjected

to HPLC to determine glycolytic intermediates. Data arepresented as mean ± SEM, n = 29 for fetal livers group of **a**, **b**, **j**, **k**, n = 24 for fetal livers fasting 24 h group of **a**, **b**, **j**, **k**; n = 23 for fetal livers group of **c**, n = 22 for fetal livers fasting 24 h group of **c**; n = 24 for fetal livers group of **d**, n = 19 for fetal livers fasting 24 h group of **d**; n = 25 for fetal livers group of **i**, n = 23 for fetal livers fasting 24 h group of **i**; n = 8 for each group of **h**, **n**; n = 7 for each group of **l**, **m**. P values were calculated using unpaired two-tailed Student's t-test (**c**, **d**, **g**, **h**, **n**), or unpaired t test with Welch's correction (**f**, **i**, **j**, **l**, **m**), or unpaired two-tailed Mann-Whitney test (**a**, **b**, **e**, **k**). ns, not significant ($P > 0.05$).

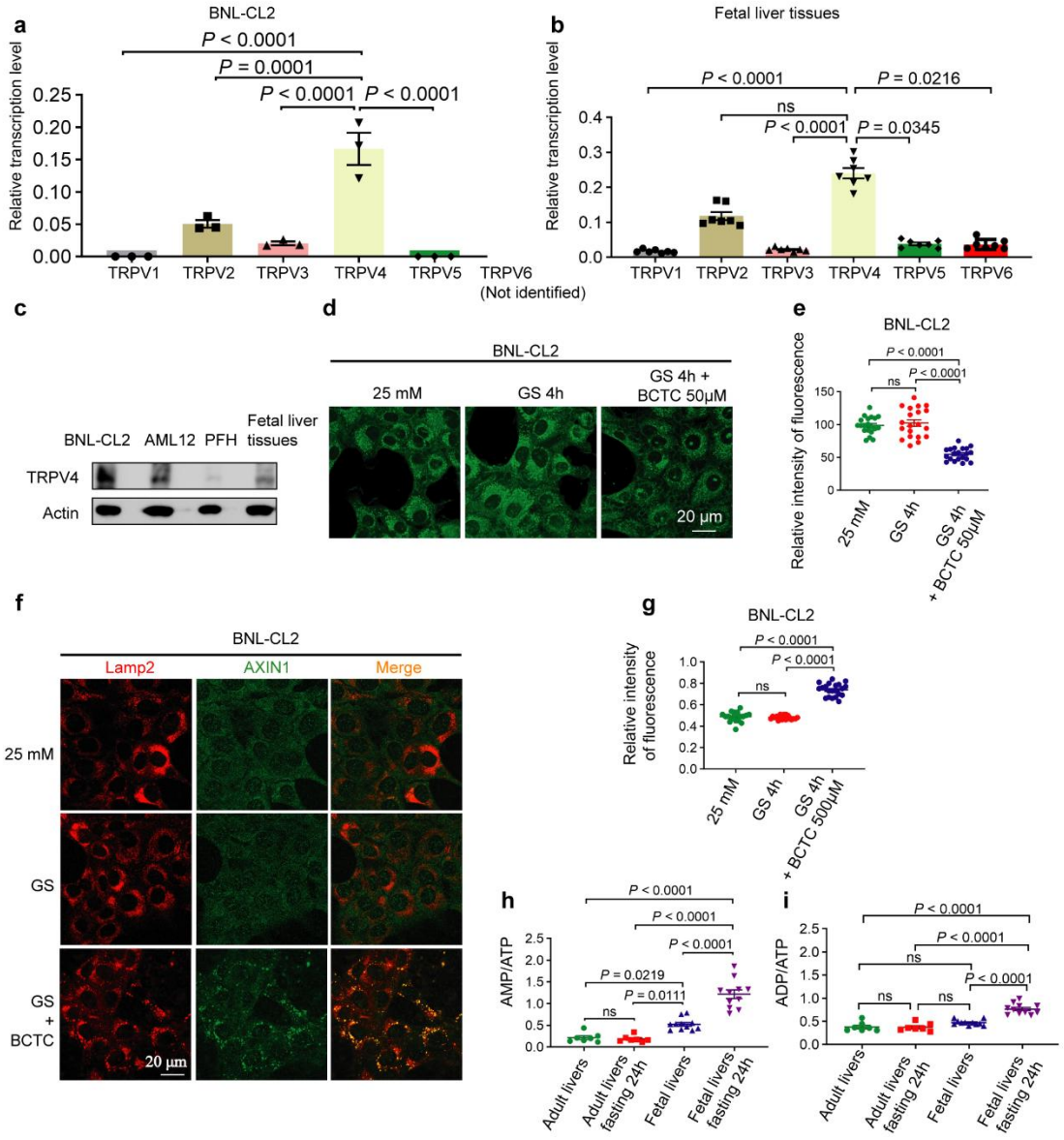

Fig. S9. Fetal AMPK is allosterically activated through the canonical, AMP-dependent mechanism, related to Fig. 3.

a TRPV4 has the highest mRNA levels in BNL-CL2 cells (by transcriptomics). Data presented as mean ± SEM, $n = 3$ for each group, with P values calculated by one-way ANOVA, followed by Dunnett's multiple comparisons test, all compared with TRPV4 group. **b** TRPV4 has the highest mRNA levels in E18.5d fetal liver (by qPCR). Data presented as mean ± SEM, $n = 7$ for each group, with P values calculated using Kruskal-

Wallis test, followed by Dunn's multiple comparisons test , all compared with TRPV4 group. **c** TRPV4 can be detected in BNL-CL2, AML12, PFH, and fetal liver tissues. **d**, **e** Forced inhibition of TRPVs in fetal hepatocytes can inhibit the activity of v-ATPase. The BNL-CL2 (**d**) was either glucose-starved (GS) or treated with 50 μM BCTC, the TRPV inhibitor, as a control + GS for 4 h. The cells were incubated with 1μM Lysosensor^{TM} Green DND-189 (Thermo L7535) for 30 min to detect the PH of lysosomes. Representative images are shown in **d**, and the relative intensity of fluorescence in **e** was presented as mean ± SEM, n = 20 for 25 mM group of **e**, n = 20 for GS 4 h group of **e**, n = 20 for GS 4 h + 50 μM BCTC group of **e**, with P values calculated using two-way ANOVA, followed by Tukey. **f**, **g** Forced inhibition of TRPVs in fetal hepatocytes by BCTC effectively triggers the lysosomal translocation of AXIN in fetal hepatocytes. BNL-CL2 cells were either glucose-starved for 4 h or treated with 500 μM BCTC, the TRPV inhibitor, for 2 h. Endogenous AXIN1 (labelled in green with goat anti-AXIN1 antibody, Santa Cruz Biotechnology SC-8567) and the lysosome marker LAMP2 (labelled in red with rat anti-LAMP2 antibody, Abcam AB13524) were then stained. Representative images are shown in **f**, and the Mander's overlap coefficients in **g** (presented as mean ± SEM, n = 20 for 25 mM group, n = 20 for GS 4 h group, n = 21 for GS 4 h + BCTC 500 μM group, with P values calculated using two-way ANOVA, followed by Tukey). **h**, **i** Glucose starvation significantly increases the ratios of AMP:ATP and ADP:ATP in fetal hepatocytes. Liver tissues were collected from pregnant mice embryos (E18.5d; fetal liver tissue) and adult mice (8-week-old; adult liver tissue), after being fasted for 0 h or 24 h. HPLC was used to detect energy

203 levels in tissues (presented as mean ± SEM, n = 7 for each adult group of **h**, **i**, n = 11

204 for each fetal group of **h**, **i** with P values calculated using two-way ANOVA, followed

205 by Tukey). The original western blots with protein ladder are shown in Supplementary

206 Data S1. ns, not significant ($P > 0.05$).

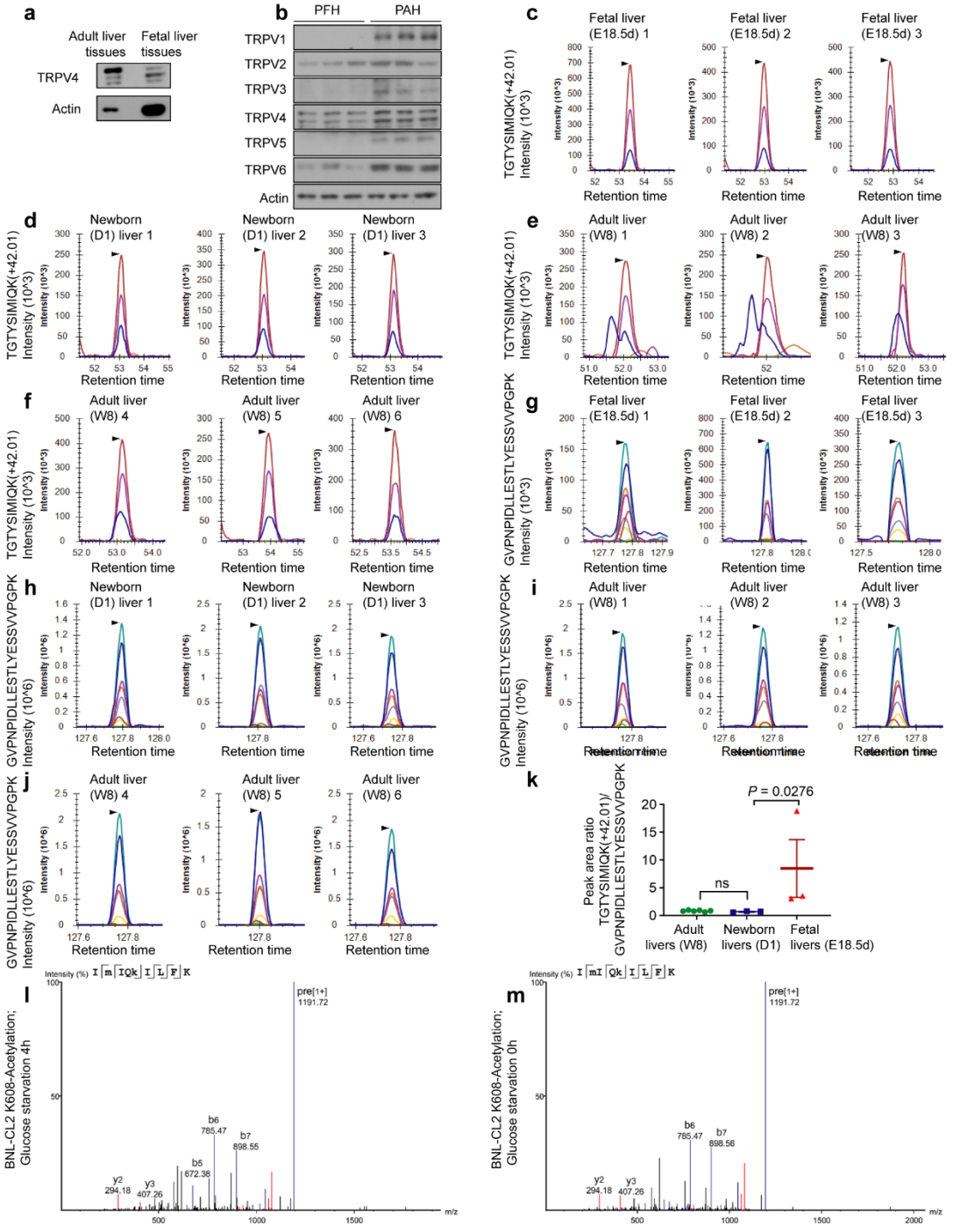

Fig. S10. Levels of acetylated TRPV4-K608 are significantly higher in the fetal liver than in the adult liver, related to Fig. 3 and Fig. 4.

a The protein level of TRPV4 in fetal liver tissues is lower than those in adult liver tissue. **b** The protein level of TRPV in PFH is lower than those in PAH. **c**–**k** Levels of

212 acetylated TRPV4-K608 are significantly higher in fetal liver than in adult liver, as
213 determined by quantitative mass spectrometry analysis. Quantitative modification mass
214 spectrometry detected a peptide segment containing K608-acetylation (TGTYSIMIQK
215 (+42.01)) and a peptide segment (GVPNPIDLLESTLYESSVVPGPK). The peak area
216 represents the relative abundance of each peptide segment in the sample. The peak area
217 ratio of TGTYSIMIQK (+42.01)/GVPNPIDLLESTLYESSVVPGPK represented the
218 relative level of acetylated TRPV4 (at K608 site) in different samples (presented as
219 mean ± SEM, n = 6 (adult livers of **k**; **e**, **f**, **i**, **j**), n = 3 (newborn livers of K; D, H), n =
220 3 (fetal livers of **k**; **c**, **g**), with P values calculated using Kruskal-Wallis test, followed
221 by Dunn's multiple comparisons test). **l**, **m** Qualitative mass spectrometry shows the
222 presence of acetylation modification at the K608 site of TRPV4 in BNL-CL2. TRPV4
223 was enriched from BNL-CL2 cells stably expressing HA-tagged TRPV4 using
224 immunoprecipitation. The original western blots with protein ladder are shown in
225 Supplementary Data S1. ns, not significant ($P > 0.05$).

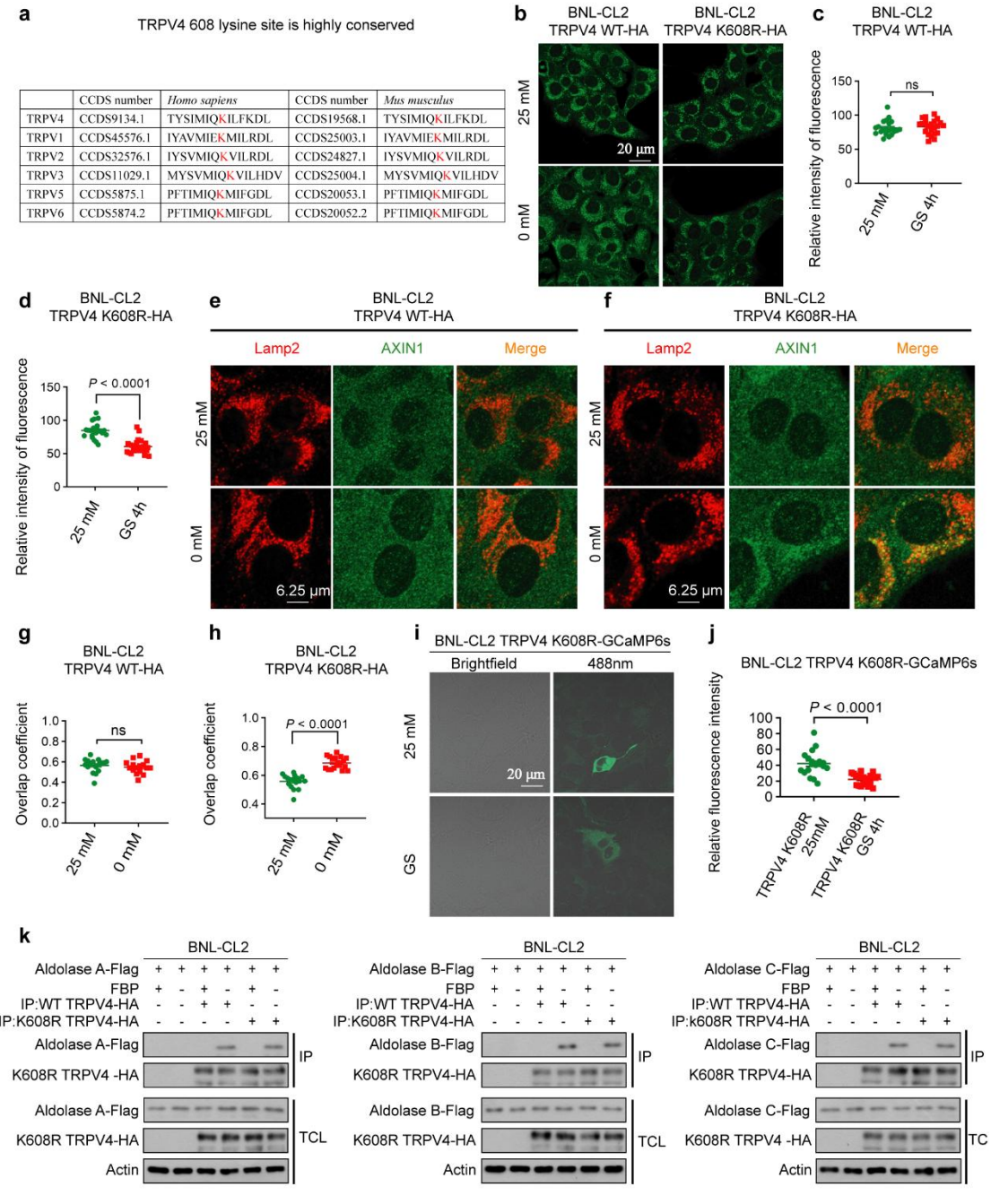

Fig. S11. Deacetylation of TRPV during intrauterine development confers sensitivity to low glucose, related to Fig. 4.

a The K608 residue is highly conserved among different species and different members of the TRPV family. **b–d** v-ATPase inhibition can be observed in fetal hepatocytes

231 expressing TRPV4-K608R in low glucose conditions, as seen in adult cells. The cells
232 were incubated with 1 μM Lysosensor^{TM} Green DND-189 (Thermo L7535) for 30 min
233 to detect the PH of lysosomes. The BNL-CL2 cells stably expressing HA-tagged
234 TRPV4 WT (left panel of **b**, **c**) or HA-tagged TRPV4 K608R (right panel of **b**, **d**) were
235 glucose-starved for 4 h. Representative images are shown in B??, and the Mander's
236 overlap coefficients in **c**, **d** (presented as mean ± SEM, n = 21 for 25mM group of **c**, n
237 = 22 for GS 4 h group of **c**, n = 23 for 25mM group of **d**, n = 24 for GS 4 h group of **d**,
238 with P values calculated using unpaired two-tailed Student's t-test) (**c**) or unpaired two-
239 tailed Mann-Whitney test (**d**)). **e**–**h** The lysosomal translocation of AXIN can be
240 observed in fetal hepatocytes expressing TRPV4-K608R in low glucose conditions. The
241 BNL-CL2 cells stably expressing HA-tagged TRPV4 WT (**e**, **g**) or HA-tagged TRPV4
242 K608R (**f**, **h**) were glucose-starved for 4 h. Representative images are shown in **e**, **f** and
243 the Mander's overlap coefficients in **g**, **h** (presented as mean ± SEM, n = 17 for 25 mM
244 group of **g**, n = 16 for 0 mM of **g**, n = 17 for 25 mM group of **h**, n = 19 for 0 mM group
245 of **h**, with P values calculated using unpaired two-tailed Student's t-test). **i**, **j** The
246 mutation of K608 does not affect the basal activity of TRPV4, but renders TRPV4 able
247 to be closed in fetal hepatocytes in low glucose conditions. BNL-CL2 cells stably
248 expressing TRPV4 K608R-GCaMP6s were glucose-starved for 4 h. TRPV4-GCaMP6s
249 were used to detect local calcium concentration, which can reflect whether TRPV4 is
250 closed or not. The intensities of the indicator were then determined. The result showed
251 that K608R-TRPV4, but not wildtype TRPV4, was closed in BNL-CL2 in low glucose
252 conditions. Statistical analysis data are shown as mean ± SEM; n = 20 for TRPV4

K608R group of **j**, $n = 20$ for TRPV4 K608R GS 4 h group of **j**; P values calculated using unpaired t test with Welch's correction (**j**). **k** The mutation of K608 of TRPV4 does not change its affinity with the FBP-unoccupied aldolase. The BNL-CL2 (fetal hepatocytes) cells stably expressing HA-tagged TRPV4 K608R and Flag-tagged aldolase were glucose-starved for 4 h. Cells were then lysed, and the lysates were incubated with 20 μM FBP for 12 h. The interaction between aldolase and TRPV4 in the lysates was then determined by immunoprecipitation of HA-tag, followed by immunoblotting. The original western blots with protein ladder are shown in Supplementary Data S1. ns, not significant ($P > 0.05$).

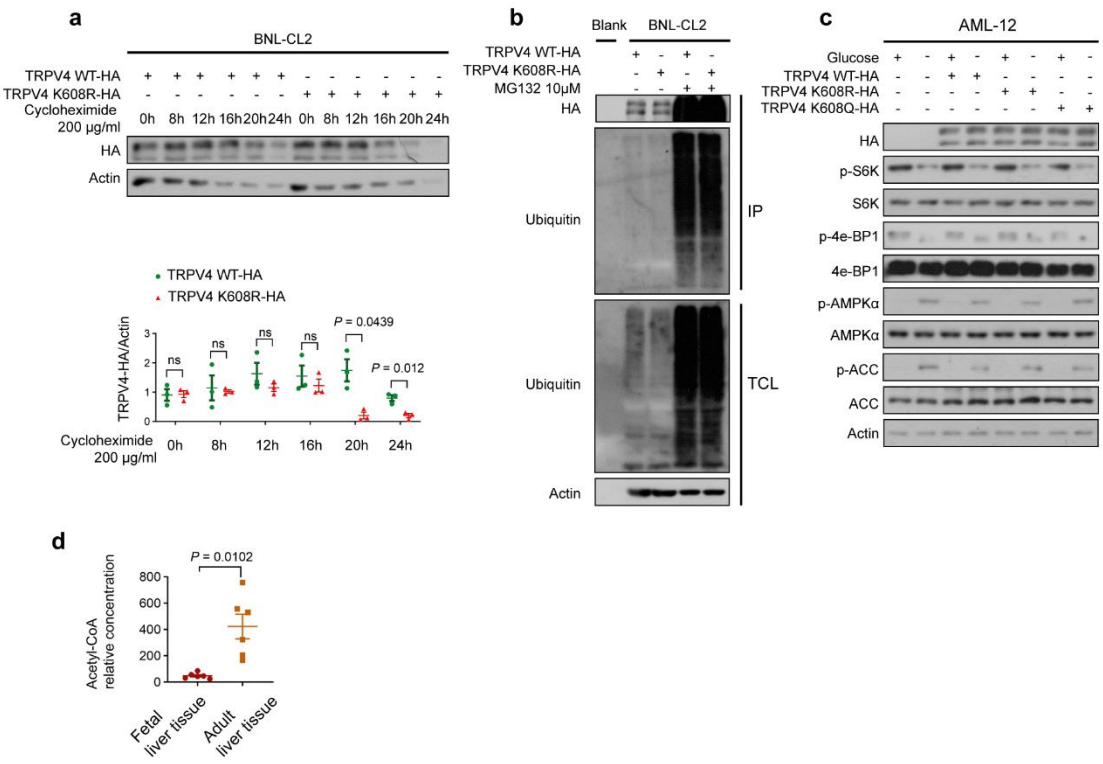

Fig. S12. Deacetylation of TRPV4 slightly decrease its protein stability, related to Fig. 4.

a, **b** The mutation of K608 of TRPV4 decreases its protein stability. BNL-CL2 (fetal hepatocytes) cells stably expressing HA-tagged TRPV4-WT or TRPV4-K608R were treated with cycloheximide (200 μg/ mL) for 0, 4, 8, 12, 16, 20 or 24 h, followed by determination of HA-tagged TRPV4 protein level by immunoblotting. Data are presented as mean ± SEM, n = 3, with P values calculated using two-way ANOVA, followed by Tukey. BNL-CL2 (fetal hepatocytes) cells stably expressing HA-tagged TRPV4-WT or TRPV4-K608R were treated with MG132 (10 μM/mL) for 24 h of **b**, followed by determination of ubiquitin (abcam, ab134953) by immunoblotting. **c** The mutation of TRPV4-K608 to Q does not change AML12 response to low glucose. The AML12 (adult hepatocytes) cells stably expressing HA-tagged TRPV4-WT, TRPV4-

K608R or TRPV4-K608Q were glucose-starved for 4 h. Cells were then lysed, followed by determination of p-S6K levels by immunoblotting. **d** The acetyl-CoA concentration in fetal mice liver tissue is lower than in the adult liver tissue. Acetyl-CoA was determined by HPLC-MS (presented as mean ± SEM, $n = 6$ for each group, with P values calculated using unpaired t test with Welch's correction). The original western blots with protein ladder are shown in Supplementary Data S1. ns, not significant ($P > 0.05$)

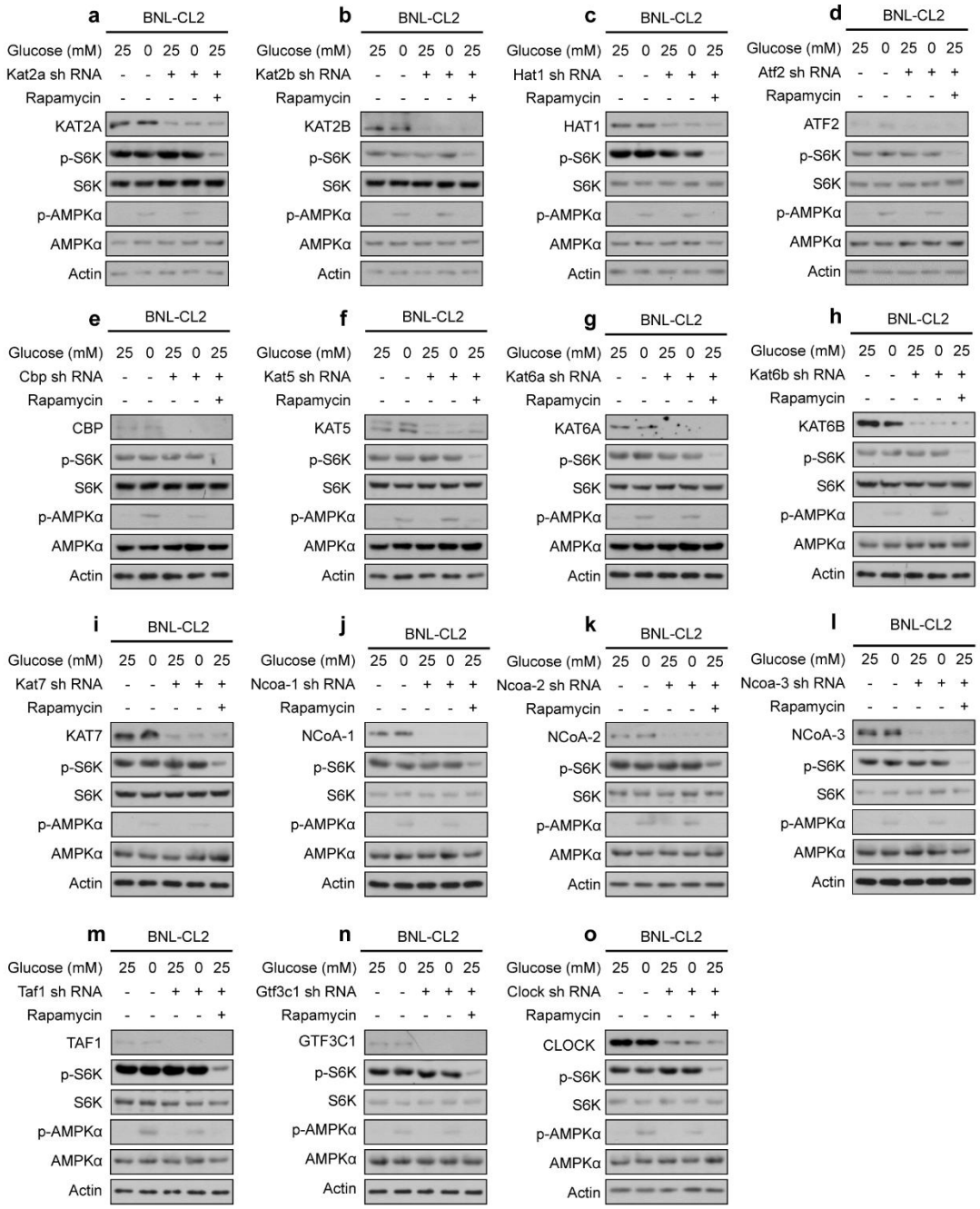

Fig. S13. Only knocking down P300 inhibits mTORC1 activity in low glucose of BNL-CL2 cells by screening all acetyltransferase, related to Fig. 4.

a–**o** The shRNA of *Kat2a*, *Kat2b*, *Hat1*, *Atf2*, *Taf1*, *Kat5*, *Kat6a*, *Kat6b*, *Kat7*, *Ncoa-1*, *Ncoa-2*, *Ncoa-3*, *TAFII250*, *Gtf3c1* and *Clock* were designed and transfected into BNL-CL2 cells by Lentivirus, respectively. Cells were under starvation for 4 h, followed by

288 determination of phosphorylation of S6K (p-S6K) levels via immunoblotting. As a
289 control, rapamycin (100 nM, treatment for 1 hour) was used to inhibit S6K
290 phosphorylation. See also phosphorylation of AMPKα in these cells. The original
291 western blots with protein ladder are shown in Supplementary Data S1.

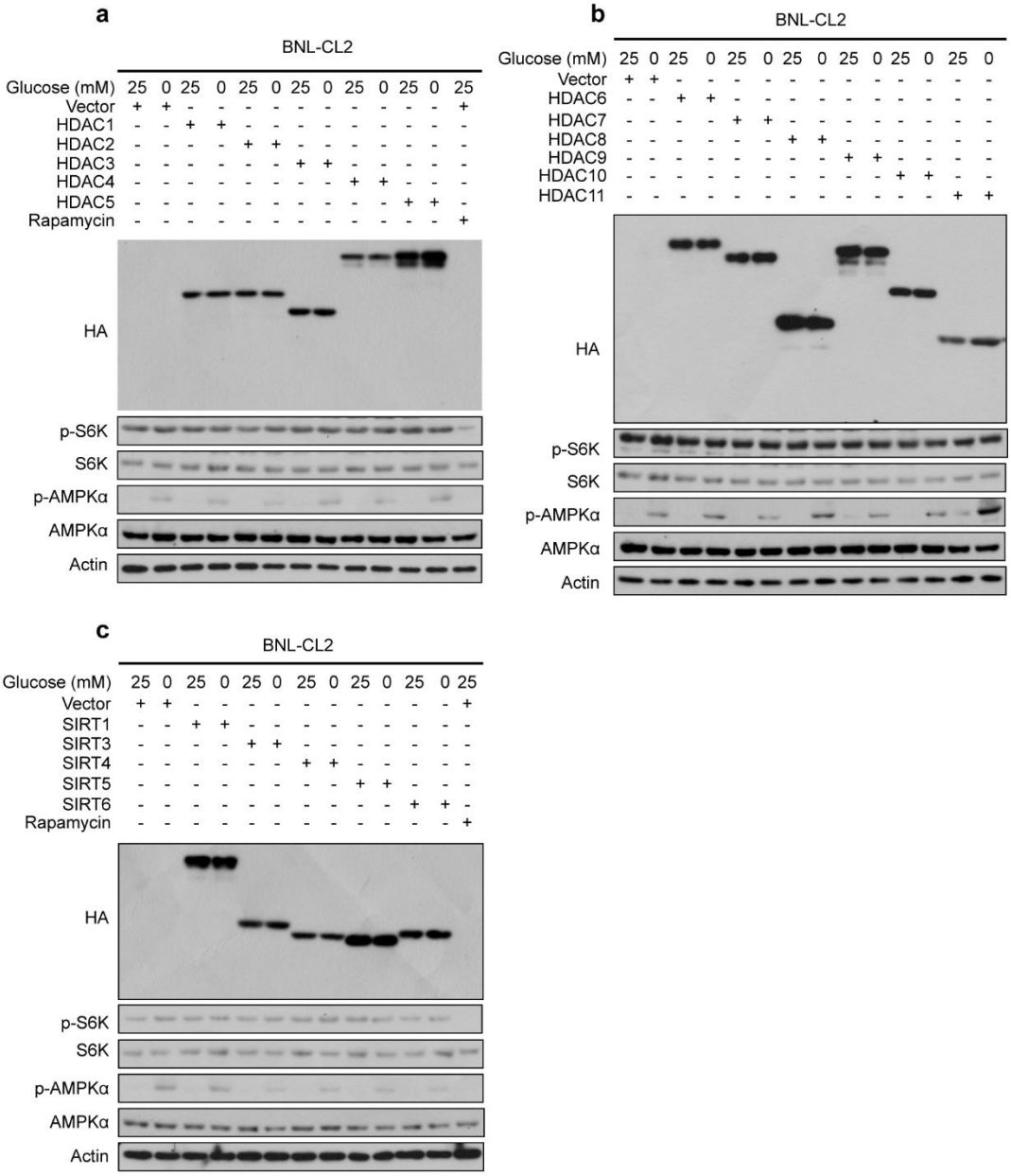

292

293 **Fig. S14. HDACs and SIRTs (expect SIRT2 and SIRT7) does not change the**

294 **mTORC1 activity in low glucose of BNL-CL2 cells, related to Fig. 4.**

295 **a**–**c** The ORF of *HDACs* (*HDAC1-HDAC11*) and *SIRTs* (*SIRT1-SIRT7*) fragments were

296 ligated into the lentivirus vector *pBOBI*, and transfected into BNL-CL2 cells by

297 lentivirus, respectively. Cells were under starvation for 4 h, followed by determination

298 of phosphorylation of S6K (p-S6K). As a control, rapamycin (100 nM, treatment for 1
299 hour) was used to inhibit S6K phosphorylation levels via immunoblotting. See also
300 phosphorylation of AMPKα in these cells. The original western blots with protein
301 ladder are shown in Supplementary Data S1.

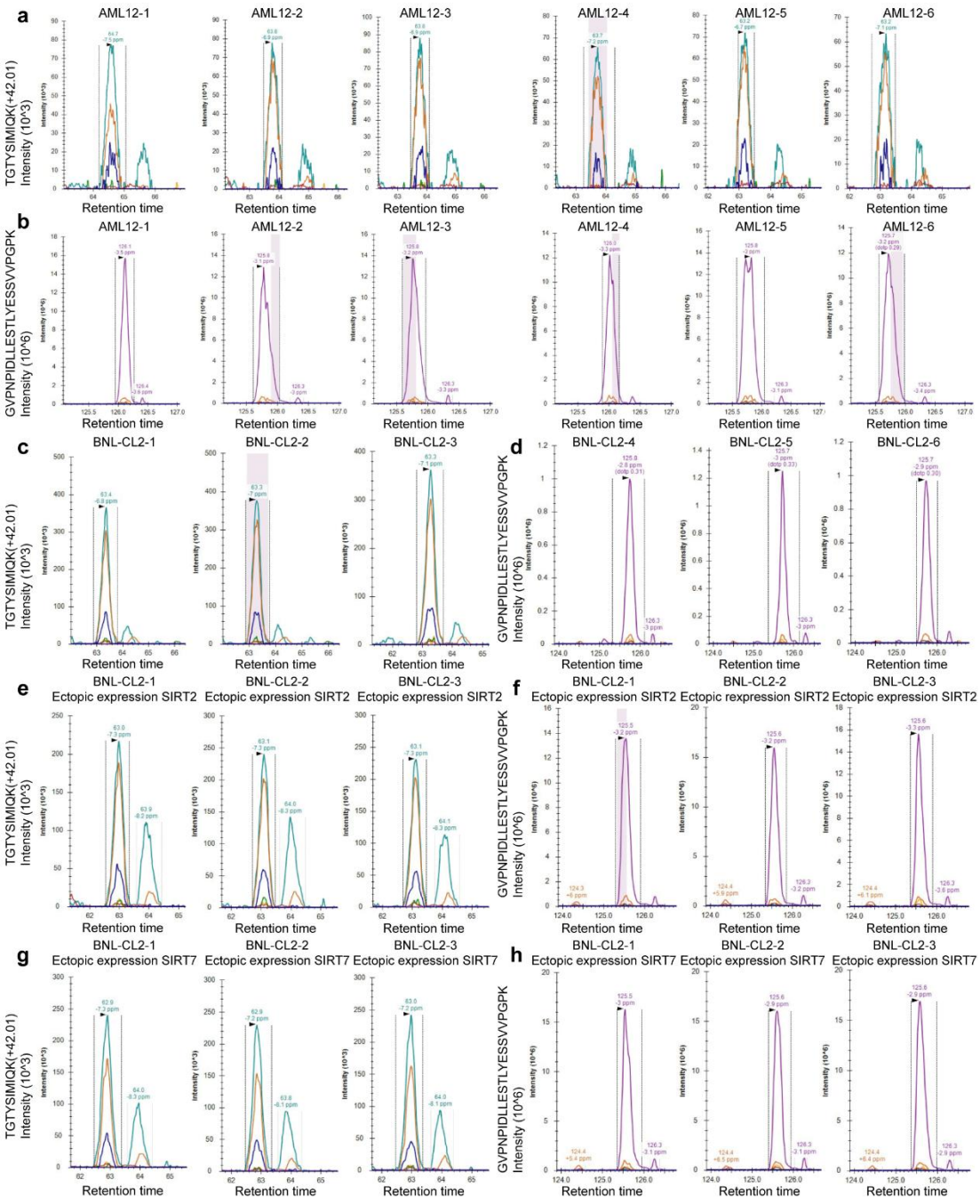

Fig. S15. Levels of acetylated TRPV4-K608 are significantly higher in the fetal liver than in the adult liver; ectopic expression of SIRT2 or SIRT7 notably reduced the levels of acetylated TRPV4-K608, related to Fig. 4.

a–**h** Levels of acetylated TRPV4-K608 are significantly higher in fetal liver than in

adult liver; ectopic expression of SIRT2 or SIRT7 notably reduced the levels of acetylated TRPV4-K608 as determined by quantitative mass spectrometry analysis. Quantitative modification mass spectrometry detected a peptide segment containing K608-acetylation (TGTYSIMIQK (+42.01)) and a peptide segment (GVPNPIDLLESTLYESSVVPGPK). The peak area represents the relative abundance of each peptide segment in the sample. The peak area ratio of TGTYSIMIQK (+42.01)/GVPNPIDLLESTLYESSVVPGPK represented the relative level of acetylated TRPV4 (at K608 site) in different samples (presented as mean ± SEM, $n = 6$ (adult livers of **a**, **b**), $n = 3$ (BNL-CL2 of **c**, **d**), $n = 3$ (ectopic expression of SIRT2 in BNL-CL2 of **e**, **f**), $n = 3$ (ectopic expression of SIRT7 in BNL-CL2 of **g**, **h**), with *P* values calculated using unpaired two-tailed Student's *t*-test is used. Qualitative mass spectrometry shows the presence of acetylation modification at the K608 site of TRPV4 in BNL-CL2. TRPV4 was enriched from BNL-CL2 cells stably expressing HA-tagged TRPV4 using immunoprecipitation.

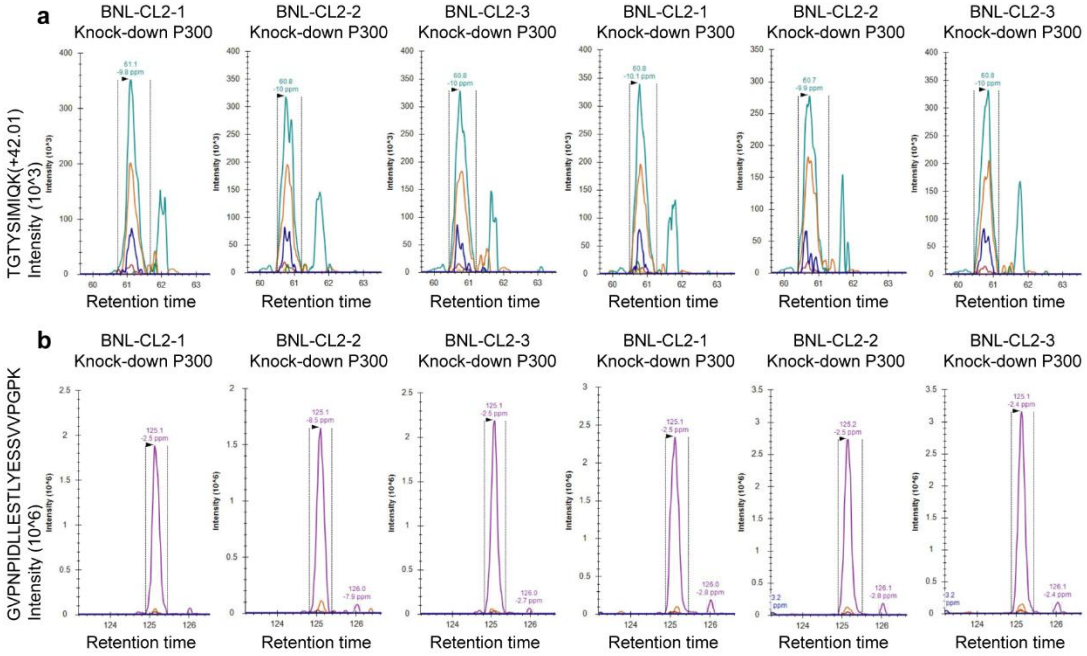

Fig. S16. Levels of acetylated TRPV4-K608 decreases significantly when P300 is knocked down in the fetal BNL-CL2 cells, related to Fig. 4.

a, **b** Levels of acetylated TRPV4-K608 are downregulated notably when P300 is knocked down in the fetal BNL-CL2 cells. shP300 significantly reduced the levels of acetylated TRPV4-K608 as determined by quantitative mass spectrometry analysis. Quantitative modification mass spectrometry detected a peptide segment containing K608-acetylation (TGTYSIMIQK (+42.01)) and a peptide segment (GVPNPIDLLESTLYESSVVPGPK). The peak area represents the relative abundance of each peptide segment in the sample. The peak area ratio of TGTYSIMIQK (+42.01)/GVPNPIDLLESTLYESSVVPGPK represented the relative level of acetylated trpv4 (at K608 site) in different samples (presented as mean ± SEM, $n = 3$ (shP300 of **a**), $n = 3$ (BNL-CL2 of **b**), with P values calculated using unpaired two-tailed Student's t-test is used. Qualitative mass spectrometry shows the presence of

335 acetylation modification at the K608 site of TRPV4 in BNL-CL2. TRPV4 was enriched

336 from BNL-CL2 cells stably expressing HA-tagged TRPV4 using immunoprecipitation.

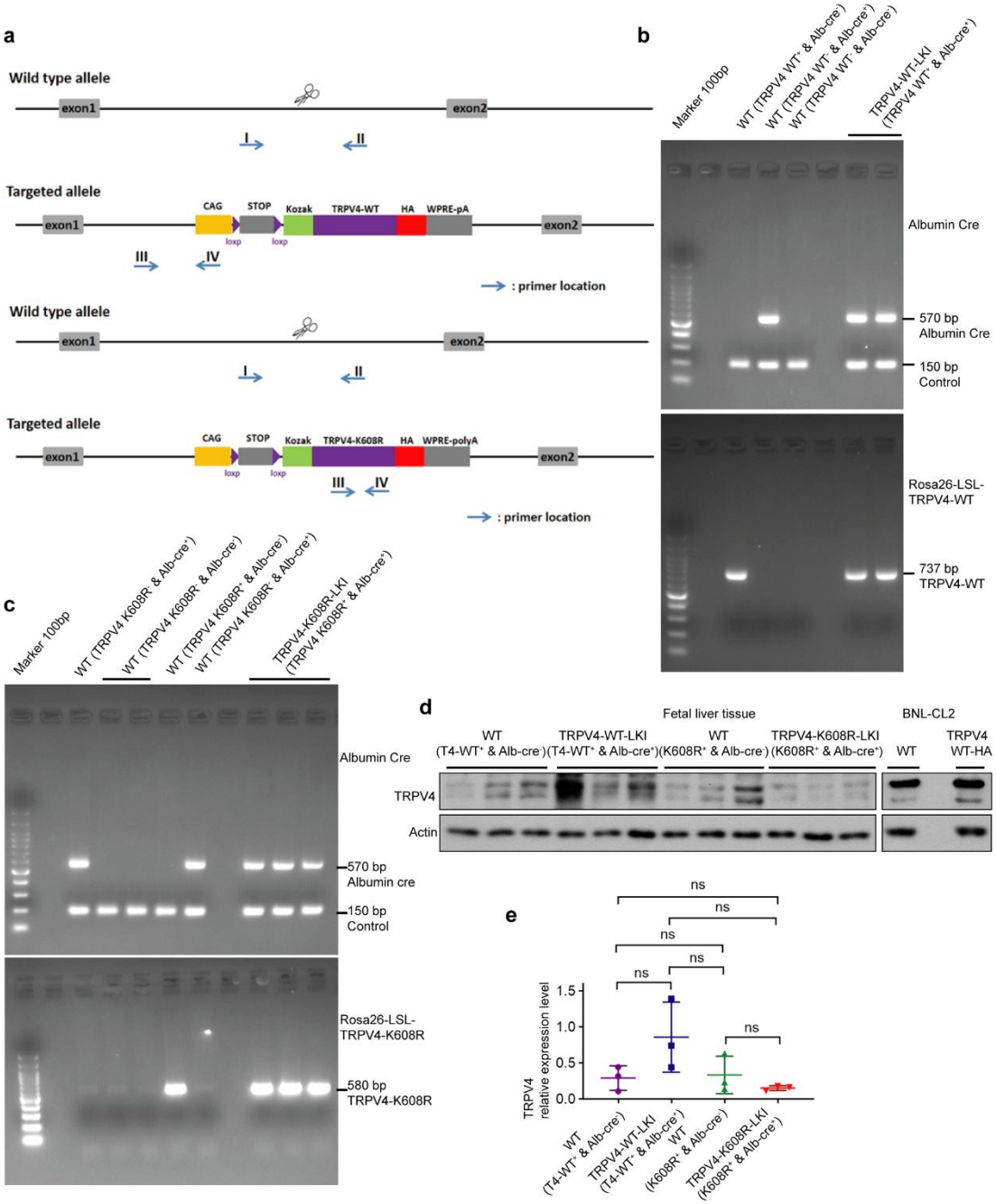

337

338 **Fig. S17. Phenotypes of fetal mice with TRPV4-K608R expression, related to Fig.**

339 **5.**

340 **a**–**c** Genotypes of fetal liver samples. **d**, **e** The knock-in of TRPV4-WT or K608R does

341 not influence TRPV4 basal protein expression in fetal livers. Liver tissues collected

342 from E18.5d fetal mice with liver-specific transgenic mice WT (T4-WT^+ & Alb-cre^-),
343 TRPV4-WT-LKI (T4-WT^+ & Alb-cre^+), WT ($K608R^+$ & Alb-cre^-) and TRPV4-K608R-
344 LKI ($K608R^+$ & Alb-cre^+). Data are shown as mean ± SEM, $n = 3$ in each group of **e**,
345 with *P* values calculated using one-way ANOVA, followed by Tukey. The original
346 western blots with protein ladder are shown in Supplementary Data S1. ns, not
347 significant ($P > 0.05$).

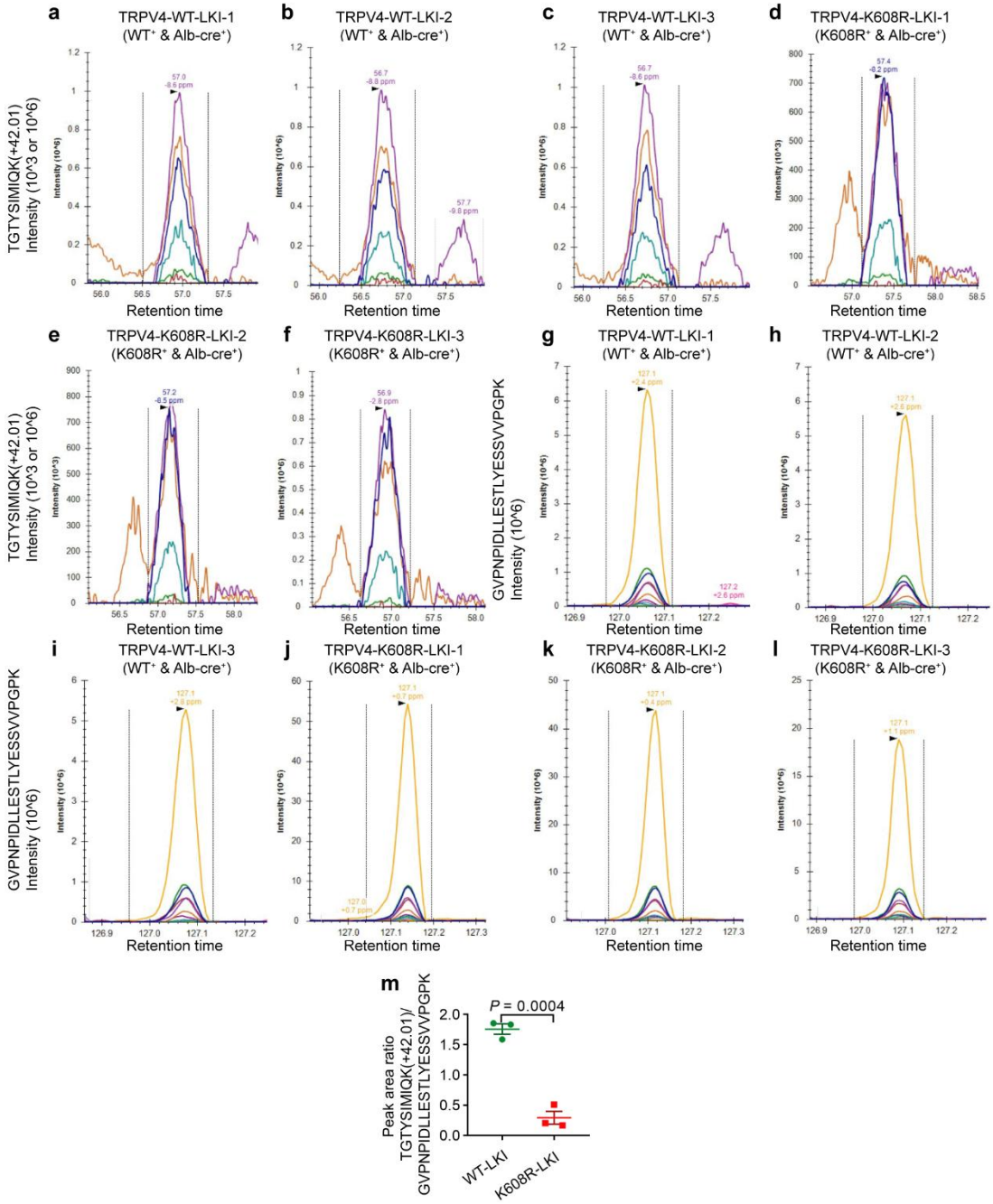

Fig. S18. Levels of acetylated TRPV4-K608 are significantly lower in the TRPV4-K608R-LKI fetal liver, related to Fig. 5.

a–**m** Levels of acetylated TRPV4-K608 are significantly higher in TRPV4-WT-LKI fetal liver than in TRPV4-K608R-LKI liver, as determined by quantitative mass spectrometry analysis. Quantitative modification mass spectrometry detected a peptide

segment containing K608-acetylation (TGTYSIMIQK (+42.01)) and a peptide segment (GVPNPIDLLESTLYESSVVPGPK). The peak area represents the relative abundance of each peptide segment in the sample. The peak area ratio of TGTYSIMIQK (+42.01)/GVPNPIDLLESTLYESSVVPGPK represented the relative level of acetylated TRPV4 (at K608 site) in different samples (presented as mean ± SEM, $n = 3$ (WT-LKI fetal livers of **a**, **b**, **c**; **g**, **h**, **i**; **m**), $n = 3$ (K608R-LKI fetal livers of **d**, **e**, **f**; **j**, **k**, **l**; **m**), with *P* values calculated using unpaired two-tailed Student's *t*-test is used).

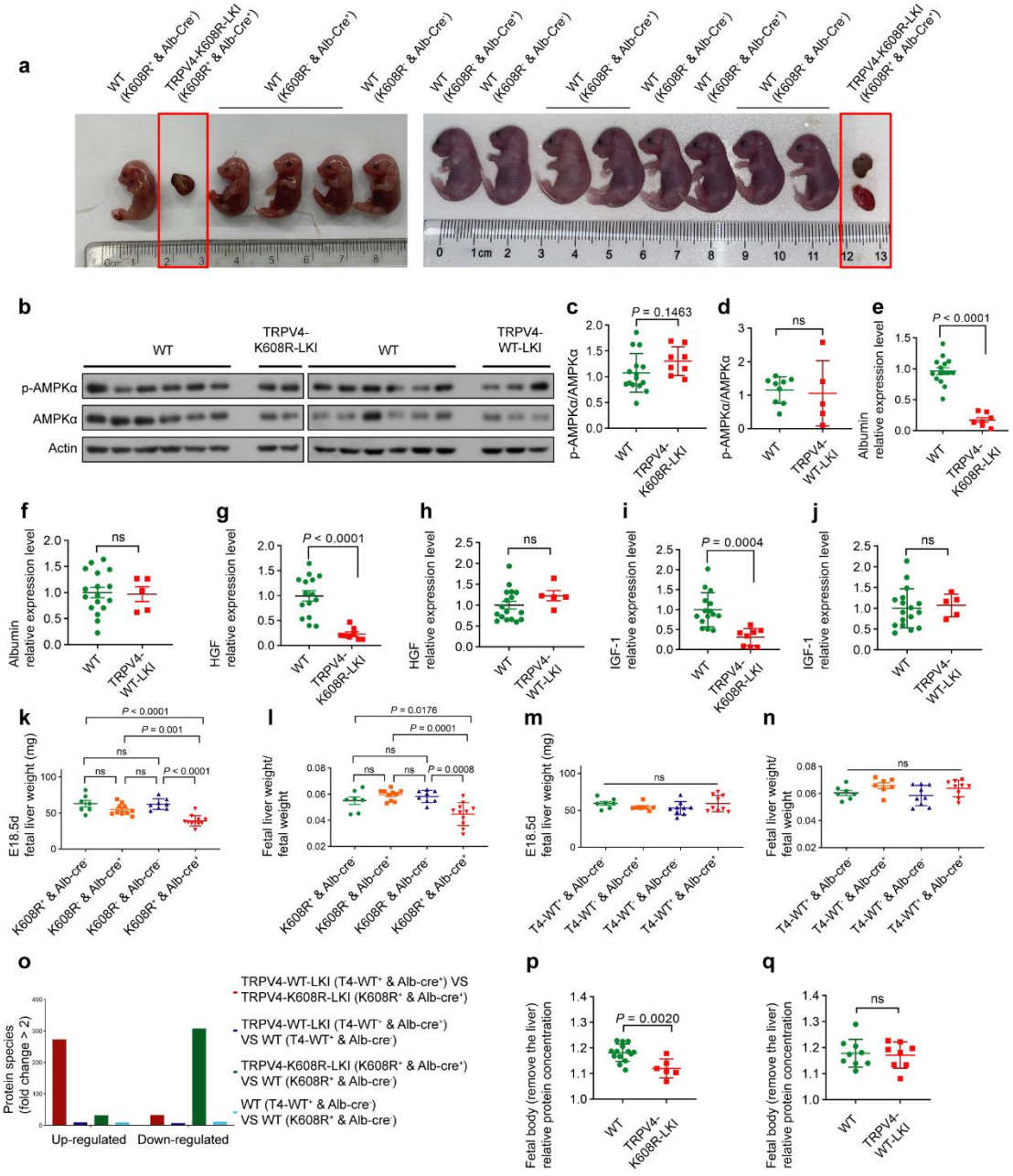

361

362 **Fig. S19. Deacetylation of TRPV4 decrease the albumin, HGF, and IGF-1 proteins**

363 **concentration in fetal hepatocytes, related to Fig. 5.**

364 **a** Approximately 18% (2/11) of embryos with specific K608R-TRPV4 expression in

365 the liver died during intrauterine development. **b**–**d** p-APMK levels showed no obvious

differences in WT and TRPV4-K608R-LKI group (**b**), and in WT and TRPV4-WT-LKI group (**b**). Data are shown as mean ± SEM, *n* = 15 for WT, *n* = 8 for TRPV4-K608R-LKI group of **c**; *n* = 9 for WT, *n* =5 for TRPV4-WT-LKI of **d** with *P* values calculated using unpaired two-tailed Student's *t*-test (**c**) or unpaired *t* test with Welch's correction (**d**). **e-j** TRPV4-K608R dominantly inhibits albumin, HGF, and IGF-1 in fetal livers. Liver tissues collected from E18.5d fetal mice with liver-specific TRPV4-K608R (Fig. 5**a**; **e**, **g**, **i**) or wildtype TRPV4 (Fig 5**b**; **f**, **h**, **j**) knocked-in were lysed, followed by determination of albumin, HGF, and IGF-1 levels by immunoblotting. Statistical analysis data are shown as mean ± SEM, *n* = 15 for WT group of **e**, **g**, **i**; *n* = 8 for TRPV4-K608R-LKI group of **e**, **g**, **i**; *n* = 17 for WT group of **f**, **h**, **j**; *n* = 5 for TRPV4-WT-LKI group of **f**, **h**, **j** with *P* values calculated using unpaired two-tailed Student's *t*-test (**e**, **f**, **i**, **j**), or unpaired *t* test with Welch's correction (**g**), or unpaired two-tailed Mann-Whitney test (**h**). **k**–**n** The fetal liver weight and the fetal liver weight/body weight of TRPV4-K608R-LKI mice decrease significantly. Data are shown as mean ± SEM, *n* = 7 for $T4\text{-}K608R^{+}$ & $Alb\text{-}cre^{-}$ of **k**, **l**, *n* = 10 for $T4\text{-}K608R^{-}$ & $Alb\text{-}cre^{+}$ of **k**, **l**; *n* = 8 for $T4\text{-}K608R^{-}$ & $Alb\text{-}cre^{-}$ of **k**, **l**, *n* = 11 for $T4\text{-}K608R^{+}$ & $Alb\text{-}cre^{+}$ of **k**, **l**; *n* = 7 for $T4\text{-}WT^{+}$ & $Alb\text{-}cre^{-}$ of **m**, **n**, *n* = 7 for $T4\text{-}WT^{-}$ & $Alb\text{-}cre^{+}$ of **m**, **n**, *n* = 9 for $T4\text{-}WT^{-}$ & $Alb\text{-}cre^{-}$ of **m**, **n**, *n* = 9 for $T4\text{-}WT^{+}$ & $Alb\text{-}cre^{+}$ of **m**, **n**, with *P* values calculated using one-way ANOVA, followed by Tukey (**k**, **l**, **n**); or using Kruskal-Wallis test, followed by Dunn's multiple comparisons test (**m**). **o** Proteomics data demonstrated that protein level decrease significantly in the TRPV4-K608R-LKI mice fetal liver tissues. The fetal liver tissues from $T4\text{-}WT^{+}$ & $Alb\text{-}cre^{-}$, $T4\text{-}WT^{+}$ & $Alb\text{-}cre^{+}$, $K608R^{+}$ & $Alb\text{-}cre^{-}$ and

388 *K608R*$^{+}$ & *Alb-cre*$^{+}$ (E18.5d) were analyzed by proteomics. **p**, **q** In addition to liver
389 abnormalities, the body protein concentration (removed the liver) of K608R-LKI fetal
390 mice decreased, while that of WT-LKI fetal mice did not decrease. Data are shown as
391 mean ± SEM, n = 14 for WT of **p**, n = 6 for *T4-K608R*$^{+}$ & *Alb-cre*$^{+}$ of **p**, **i**; n = 9 for
392 WT of **q**, n = 8 for *T4-WT*$^{+}$ & *Alb-cre*$^{+}$ of **q**, with P values calculated using unpaired
393 two-tailed Student's t-test. The original western blots with protein ladder are shown in
394 Supplementary Data S1. ns, not significant ($P > 0.05$).

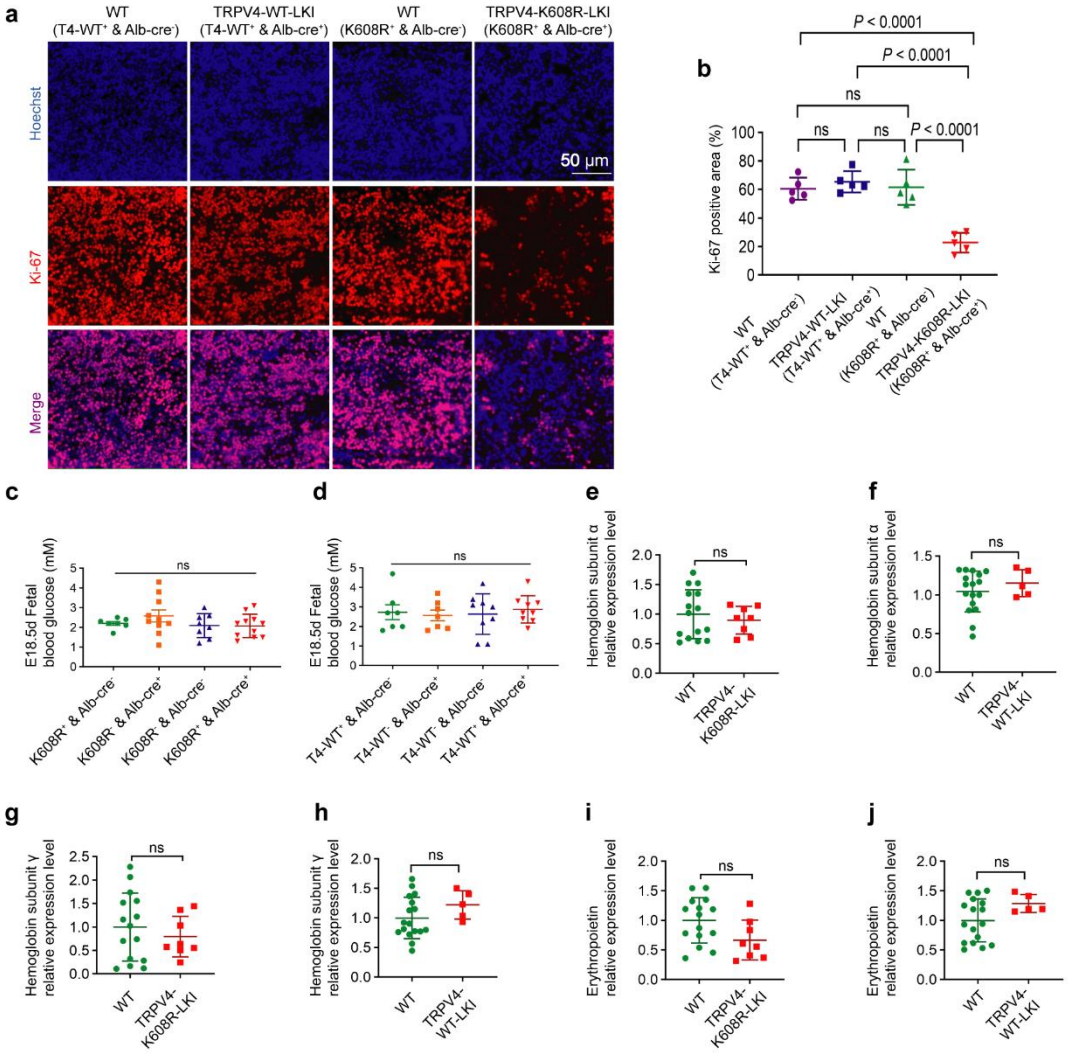

Fig. S20. Deacetylation of TRPV4 has little effect on liver hemoglobin, liver erythropoietin and blood glucose levels in fetus, but decrease the proliferation rate in fetal hepatocytes, related to Fig. 5.

a, **b** The knockin of TRPV4-K608R significantly decreases fetal hepatocytes proliferation in liver tissue. Liver tissues collected from E18.5d fetal mice with liver-specific transgenic mice WT (*T4-WT*$^{+}$ & *Alb-cre*$^{-}$), TRPV4-WT-LKI (*T4-WT*$^{+}$ & *Alb-cre*$^{+}$), WT (*K608R*$^{+}$ & *Alb-cre*$^{-}$) and TRPV4-K608R-LKI (*K608R*$^{+}$ & *Alb-cre*$^{+}$). Data are shown as mean ± SEM, $n = 6$ in each group of **b**, with P values calculated using

404 one-way ANOVA, followed by Tukey. **c**, **d** TRPV4-K608R has little effect on fetal
405 blood glucose levels. Data are shown as mean ± SEM, $n = 7$ for *T4-K608R*$^{+}$ & *Alb-cre*$^{-}$
406 of **c**, $n = 10$ for *T4-K608R*$^{-}$ & *Alb-cre*$^{+}$ of **c**; $n = 8$ for *T4-K608R*$^{-}$ & *Alb-cre*$^{-}$ of **c**, $n = 11$
407 for *T4-K608R*$^{+}$ & *Alb-cre*$^{+}$ of **c**; $n = 7$ for *T4-WT*$^{+}$ & *Alb-cre*$^{-}$ of **d**, $n = 7$ for *T4-WT*$^{-}$ &
408 *Alb-cre*$^{+}$ of **d**, $n = 9$ for *T4-WT*$^{-}$ & *Alb-cre*$^{-}$ of **d**, $n = 9$ for *T4-WT*$^{+}$ & *Alb-cre*$^{+}$ of **d**, with
409 *P* values calculated using one-way ANOVA, followed by Dunnett's T3 multiple
410 comparisons test (**c**) or Tukey (**d**). **e**–**j** TRPV4-K608R has little effect on hemoglobin
411 and erythropoietin levels. Liver tissues collected from E18.5d fetal mice with liver-
412 specific TRPV4-K608R (Fig. 5**a**; **e**, **g**, **i**) or wildtype TRPV4 (Fig. 5**b**; **f**, **h**, **j**) knocked
413 in were lysed, followed by determination of hemoglobin α/γ and erythropoietin levels
414 by immunoblotting. Statistical analysis data are shown as mean ± SEM, $n = 15$ for WT
415 group of **e**, **g**, **i**; $n = 8$ for TRPV4-K608R-LKI group of **e**, **g**, **i**; $n = 17$ for WT group of
416 **f**, **h**, **j**; $n = 5$ for TRPV4-WT-LKI group of **f**, **h**, **j** with *P* values calculated using unpaired
417 two-tailed Student's *t*-test. ns, not significant ($P > 0.05$).

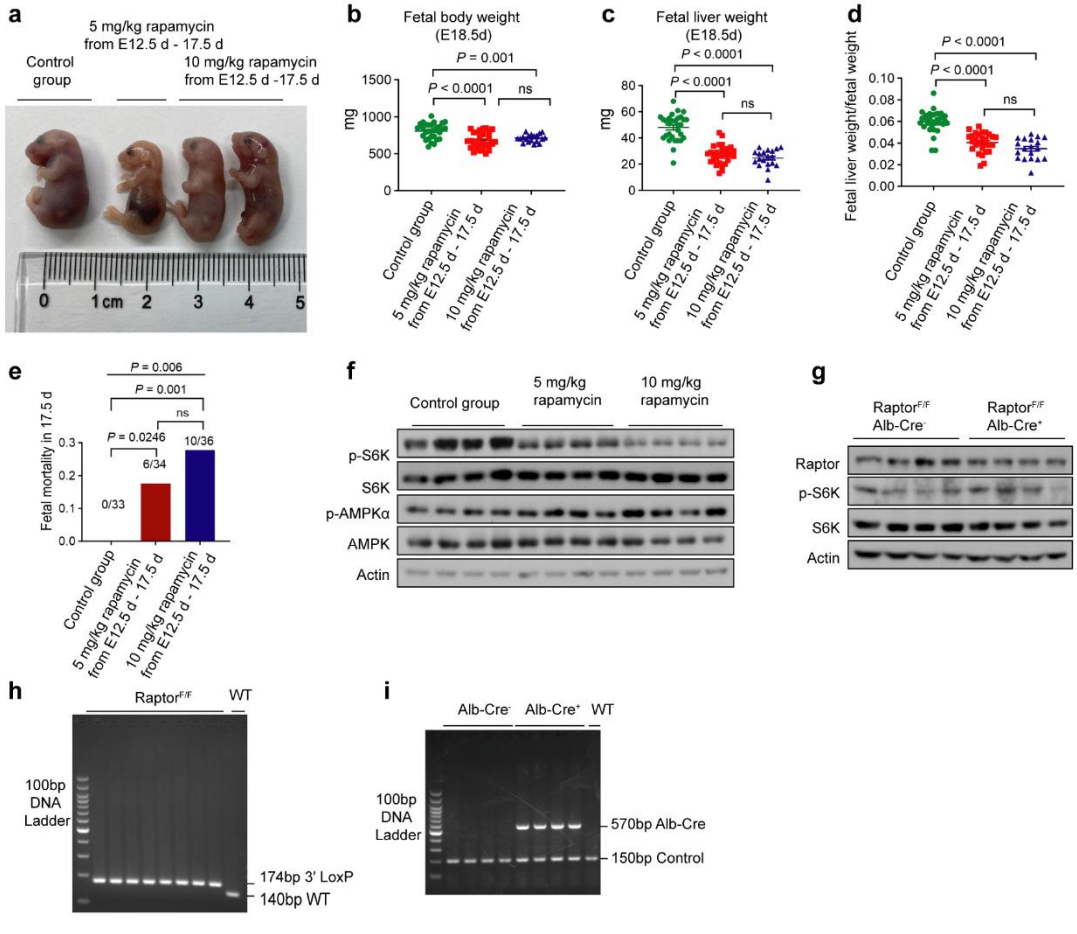

Fig. S21. Rapamycin administration in wild-type embryos, which inhibits mTORC1 in fetal livers, recapitulates the phenotypes observed in the K608R-TRPV4-expressing embryos, related to Fig. 5.

a–**e** Rapamycin administration in wild-type embryos resembles the phenotypes observed in the K608R-TRPV4-expressing embryos. Rapamycin leads to a decrease in liver weight (**c**), fetal liver weight/fetal weight (**d**), and an increase in intrauterine mortality rate (**e**) in fetal mice. Statistical analysis data are shown as mean ± SEM, *n* = 30 for control group of **b**–**d**, *n* = 28 for 5 mg/kg rapamycin group **b**–**d**, *n* = 19 for 10 mg/kg rapamycin group of **b**–**d**; *n* = 33 for control group of **e**, *n* = 34 for 5mg/kg rapamycin group of **e**, *n* = 36 for 10 mg/kg rapamycin group of **e**, with *P* values

calculated using one-way ANOVA, followed by Dunnett's T3 multiple comparisons test (**b**), Tukey (**c**) or using Kruskal-Wallis test, followed by Dunn's multiple comparisons test (**d**), or Pearson chi-square (**e**, whole group, comparison between 5mg/kg rapamycin group and 10 mg/kg rapamycin group), or followed by Fisher's exact test (**e**, comparison between control group and 5mg/kg rapamycin group, comparison between control group and 10mg/kg rapamycin group). **f** Rapamycin administration in wild-type embryos inhibits mTORC1 in fetal livers, as assessed by the p-S6K levels via immunobloting. **g** Blockage of the mTORC1 signaling by knocking out Raptor in the fetal liver is unsuccessful. The protein levels of Raptor remained mostly unaffected in the fetal liver ($Raptor^{F/F}$ & $Alb\text{-}cre^{-}$ vs $Raptor^{F/F}$ & $Alb\text{-}cre^{+}$). **h**, **i** Genotyping of $Alb\text{-}cre^{-}$, $Raptor^{F/F}$ and $Alb\text{-}cre^{+}$, $Raptor^{F/F}$ fetal mice. $Alb\text{-}cre^{+}$, $Raptor^{F/-}$ male mice were mated with $Raptor^{F/F}$ female mice to obtain $Raptor^{F/F}$ & $Alb\text{-}cre^{-}$, $Raptor^{F/F}$ & $Alb\text{-}cre^{+}$ fetal mice. The original western blots with protein ladder are shown in Supplementary Data S1. ns, not significant ($P > 0.05$).